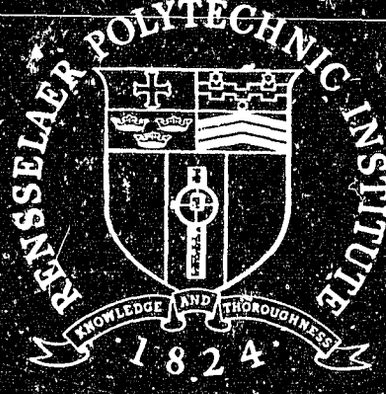

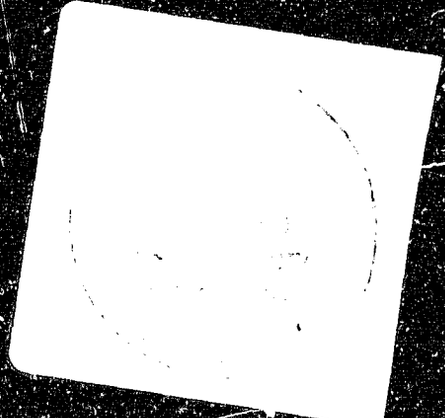

Rensselaer Polytechnic Institute

Troy, New York 12181

RPI TECHNICAL REPORT MP-69

DESIGN OF A DYNAMIC TEST PLATFORM FOR AUTONOMOUS ROBOT VISION SYSTEMS

by

Gary C. Rich

A Study Supported by the

NATIONAL AERONAUTICS AND SPACE ADMINISTRATION

under

Grant NSG-7369

and by the

JET PROPULSION LABORATORY

under

Contract 954880

School of Engineering
Rensselaer Polytechnic Institute
Troy, New York

August 1980

CONTENTS

LIST OF FIGURES

ACKNOWLEDGEMENT

I wish to express my appreciation to a few people for the immeasurable support I received during my time on the Mars Rover Project at RPI. Dr. Stephen Yerazunis was a colossal inspiration as principal investigator. His influence at RPI is wide-spread and enduring. Dr. Dean Frederick offered great amounts of both direction and confidence when they were most needed. Thomas Robison I thank endlessly for his wisdom, insight, months of work, and most of all, his friendship and companionship. Lastly I thank my wife Ruth, who was always supportive and patient, and saw to it that the dynamic test platform and this paper became reality.

ABSTRACT

This paper deals with the concept and design of a dynamic test platform for development and evaluation of a robot vision system. The platform is to serve as a diagnostic and developmental tool for future work with the RPI Mars Rover's multi-laser/multi-detector (ML/MD) vision system.

The platform allows testing of the vision system while its attitude is varied, statically or periodically. The vision system is mounted on the test platform. It can then be subjected to a wide variety of simulated Rover motions. The performance of the system in these dynamic situations can thus be examined in a controlled, quantitative fashion.

This report covers defining and modeling Rover motions and designing the platform to emulate these motions. Individual aspects of the design process are treated separately, as structural, driving linkages, and motors and transmissions.

PART 1

INTRODUCTION

1.1 The RPI Mars Rover Project

The early history of the RPI Mars Project was very diversified. Early work concerned not only roving vehicles, but orbital studies, landing modes and planetary studies. In the area of roving vehicles, much time was devoted to quantifying the many governing parameters such as expected terrain characteristics and soil compositions. Goals of a Martian mission were evaluated, including the duration of such a mission, energy requirements, the science to be conducted, the amount and type of active payload to be carried, and the means required for accomplishing these goals.

There have been a multitude of different concepts of what a planetary rover should be and do, and several shifts of emphasis on the varied aspects of rover design. At RPI, some early studies were devoted largely to the packaging/deployment question. As the Viking aeroshell was envisioned as the descent module for the Rover, the engineers devised methods of collapsing the rover to fit within the aeroshell envelope. This was an important aspect of many alternative design proposals, as well as several prototypes, and is typical of early design considerations whose importance has faded in the light of the current research goals of the project.

Mobility studies have been the subject of a great deal of rover research at RPI and elsewhere over the years. Tractive devices such as the Lockheed elastic loopwheel concept have been examined at

length. One Lockheed rover design utilized loopwheel units as the sole suspending elements on an otherwise rigid rover. Loopwheels also find use on a current rover design by the Jet Propulsion Laboratory, with articulated legs carrying the propulsion units. Martin Marietta, among others, has studied segmented rovers consisting of two or three modules, each having its own suspension/propulsion systems, be they conventional wheels or a variation on the loopwheel theme. A Cornell University rover used two major modules connected by members of limited flexibility, creating a semi-rigid vehicle structure which would bend and twist over irregular terrain.

The present RPI rover design is a rigid vehicle using four wheels, torsion-sprung at the rear, with a beam axle at the front, free to pivot about the vehicle's longitudinal axis. The origin of this design was what was commonly referred to as the "dragster concept" rover. In this, the front wheels would be lightly loaded and unpowered. In the event of very tightly constraining terrain obstacles, the front wheels could actually be lifted clear of the ground by shifting the vehicle's center of mass. This allowed the rover to pivot on its two rear wheels and a tail-mounted caster. This is another capacity which no longer furthers the goals of the project, and has hence been abandoned on the most recent RPI rover designs.

The central issue of concern for the Mars rover project has become the autonomous roving problem, or more specifically, hazard detection and obstacle avoidance. Numerous systems on the present rover are devoted exclusively to achieving these capabilities including the

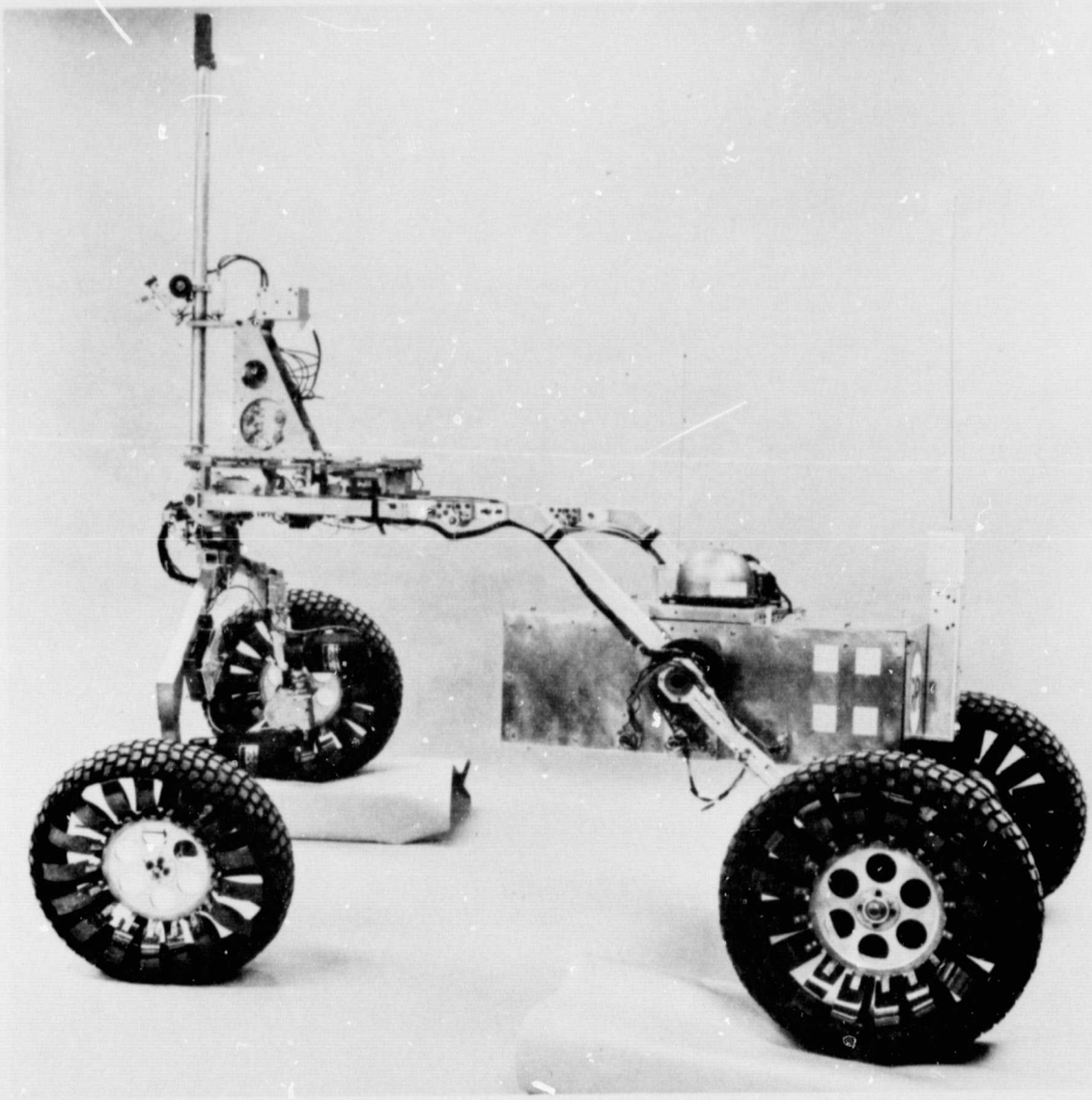

RENSSELAER AUTONOMOUS ROVING VEHICLE

Fig. 1.1

vision system and on-board course and attitude computations.

1.2 Autonomous Roving and Hazard Detection

The objective of the hazard detection system is to allow safe travel of the Mars rover in the presence of boulders, crevasses, steep slopes and the like without need for continuous guidance from Earth. After examining photographic data on the landing site area, Earth-bound scientists can instruct the rover on its gross course. This command could be either a heading and distance, or origin-to-destination instruction. It then becomes the responsibility of the on-board vision system to supply detailed information to the rover's computer, allowing intelligent and prudent short-range path selection.

To accomplish this, the vision system must first locate and characterize terrain features. It must provide information leading to proper identification of hazardous terrain, and selection of preferred paths. The RPI project has used and continues to develop discrete-point vision, permitting accurate scaling of features without the ambiguity of fringing techniques. Flexibility is afforded in data density, and new developments will allow relative desirability judgements to be made on several alternate courses of action presented.

To best exploit the vision system data, there is a full complement of decision-making algorithms for course computation. Courses are derived from information of hazards ahead, hazards behind, instantaneous vehicle attitude, steering angle, and desired heading. Based on this information, a best course decision is made. Following negotiation of a given obstacle, the controlling software endeavors to

direct the rover back to its previous desired heading, or toward its original destination.

1.3 The Single Laser/Single Detector Hazard Detection System

The first-generation hazard detection system employed on the RPI rover was the single laser/single detector system (SL/SD). The concept behind its operation is to scan 15 different azimuths, originating at the front axle center, with approximately 12° between azimuths. At each azimuth it is determined whether the terrain falls within the limits of safe passage.

A pulsing laser is fired from the top of a mast to the ground at a fixed elevation angle, such that the hit would be at 1.5 m. ahead of the rover on level ground. A photo-detector, mounted lower on the same mast, "looks" for the laser shot on the ground. The optics for this detector element include a slit iris to allow trimming the element's cone of vision in the vertical plane. With the cone centered on level ground at 1.5 m., its vertical spread is adjusted to exclude those laser hits outside 0.25 m. above or below ground level.* The output of the photo-detector is a pulse return, indicating terrain within the limits acceptable for rover travel. No return from the detector means the laser has hit outside the cone of vision, and the terrain is therefore unsafe.

Experience with the SL/SD system has shown largely acceptable performance. In a laboratory situation, with flat floor and well-

*Hazard size is here assigned as 0.25 m. height, the radius of the rover's wheels, and hence the theoretical maximum climbable step.

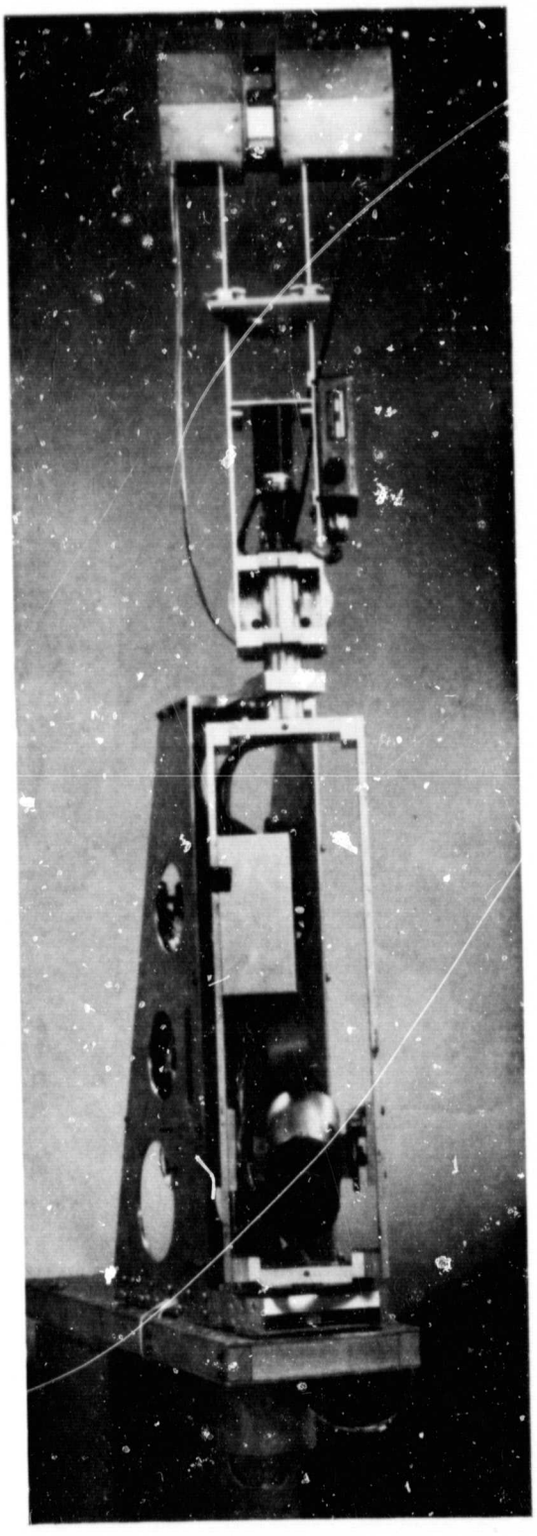

ELEVATION SCANNING MAST - FRONT VIEW

Fig. 1.2a

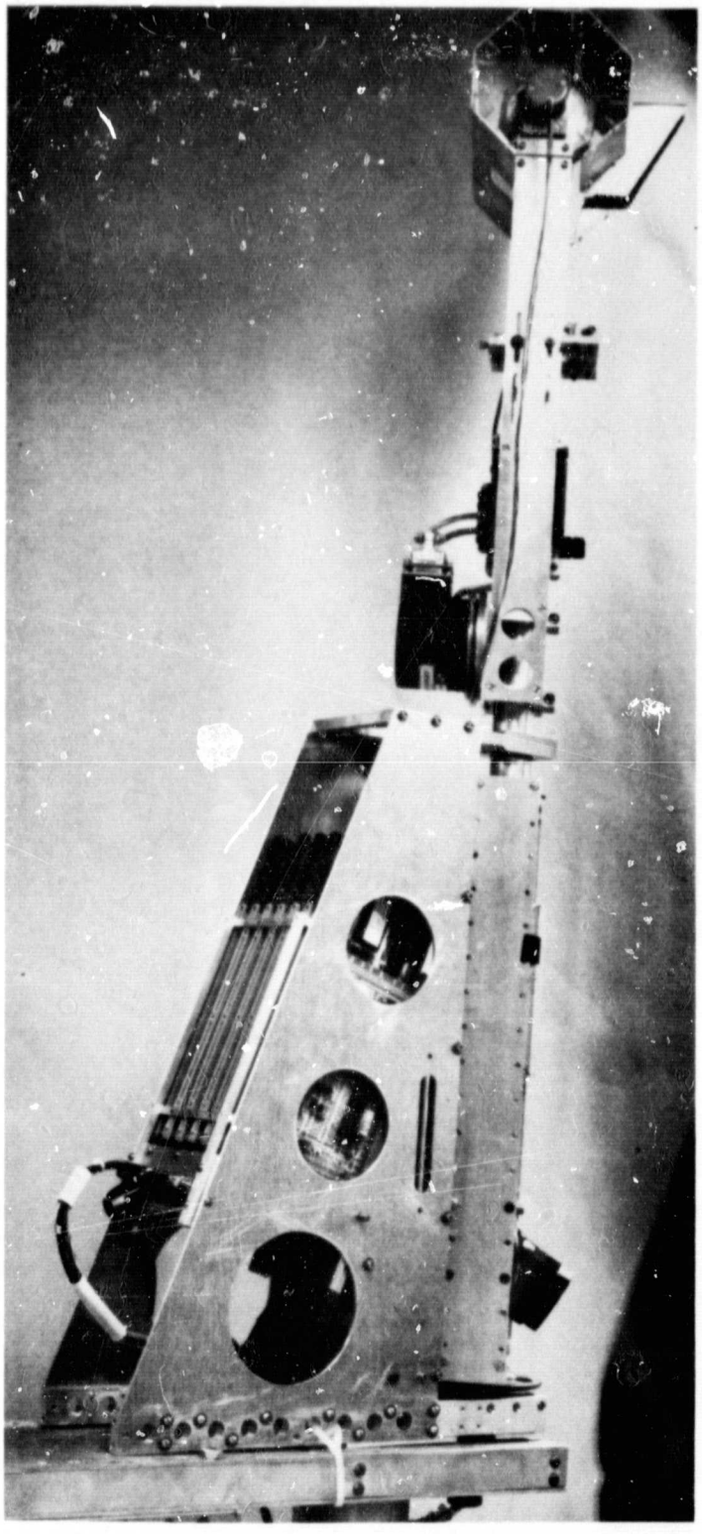

ELEVATION SCANNING MAST - SIDE VIEW

Fig. 1.2b

defined obstacles such as boxes and barrels, it was not difficult for the SL/SD to make appropriate avoidance decisions, since anything detected (i.e., any no-return situation) was to be avoided. In field testing, however, with varying gradients, random obstacles and different surface conditions under each wheel, the SL/SD performance proved more marginal. Clearances were occasionally misjudged, as were slopes and obstacles on slopes.

Confusion results partly from the single constant elevation angle, yielding only a narrow band of information, the low density of the data points, which requires excessive conservatism in choosing safe paths, and a complete lack of knowledge of anything outside the safe range for a level trajectory. A superior vision system would scan a full range of elevation angles at far greater density. The data would then describe the terrain under examination, and offer extended views when the rover is at less than ideal scanning attitudes. The information relayed to the computer would be descriptive data, as opposed to the yes/no signal of the SL/SD system.

1.4 The Multi-Laser/Multi-Detector Hazard Detection System

The second-generation rover vision system employs the advancements outlined above. Dubbed the "elevation scanner," it is similar in concept but much higher in sophistication than the SL/SD it supersedes. The mast in this case rotates continuously rather than oscillating as with the SL/SD. The number of azimuths to be scanned can be varied, with present thinking being 32 azimuths over a total of 200° to 240° (6.25° to 7.5° between azimuths). At each azi-

muth a high-frequency laser pulses, not at a fixed elevation angle, but rather onto the peripheral faces of a rotating octagonal mirror. As one of the mirror's eight faces swings past horizontal at the bottom, the laser starts firing bursts at the face, and continues to do so until the same mirror face reaches 45° to the vertical. In this way, a line of laser shots is produced covering elevation angles from nearly vertical to horizontal. The number and spacing of shots on any given azimuth are variable, with current thinking here being 32 shots at roughly 2.5° between shots. Producing a similar line of shots at each of the azimuths yields a 32 x 32 array, i.e., 1024 laser shots in space.

The detector for the elevation scanner, or ML/MD, is not a single sensor, as with the SL/SD, but a multiple-element array. Two units are currently undergoing development, one a 20-element, the other a 1024-element charge coupled device. Either of these will be used behind a lens system, the geometry of which will yield a field of view of 30° to 60° vertical. At each azimuth, the laser shots hit the ground within this envelope. The image of each laser shot is refracted by the detector optics, and sensed by one or more of the detector elements.* Given the position of the octagonal mirror when

*There is an as yet unresolved question concerning missing returns, i.e., a laser shot not being sensed by any detector element. This could indicate: a) a steep drop, such that there is no ground inside the detector envelope within the range of interest, 0 to 4 m.; b) an overhang, which is highly unlikely to be encountered and would certainly be a hazard if it were; c) an obstacle of height and depth such that it obscures the laser hit from the detector. This is one of the situations to be studied in this program.

a given shot is fired (and hence the elevation angle of that shot), which element of the detector array senses the shot (hence the angle of the reflection), and the distance between the mirror and the detector, the position of the hit may be determined by triangulation. This point defines a terrain segment. When this definition is made for each of 32 shots on each of 32 azimuths, a three-dimensional terrain map is produced.

A detailed description of the terrain ahead is thus given, relative to the rover frame of reference. The question then becomes: what happens to this data when the rover frame differs from the planetary frame, either by constant angular displacements or by some time-varying rotations? Put differently, what if the rover is traveling irregular terrain?

Due to the random nature of rover behavior on uneven surfaces, little stands to be gained by conducting autonomous roving experiments without first performing exhaustive quantitative studies into the ML/MD's performance in various static and dynamic states. This is the impetus behind the dynamic test platform program.

The purposes of the platform program are to quantitatively test the data grid of the elevation scanner system and to verify and optimize the sophisticated hardware and software utilized. This will be accomplished by constructing a test terrain mock-up, and using the platform, subjecting the elevation scanner to the type of motion it would experience on the rover. Comparing known terrain specifications with data from the ML/MD as it scans the mock-up, proper interpretation and handling of the data can be derived.

PART 2

THE DYNAMIC TEST PLATFORM CONCEPT

The dynamic test platform mechanically emulates rover behavior on irregular terrain surfaces. By the design of the platform, it is possible to subject the elevation scanner to many various attitudes and motions. These are similar to the perturbations it would experience if mounted on the rover as the latter negotiates irregular ground. The advantage is that the perturbations are predetermined and controllable. This enables studying the ML/MD's performance characteristics without the randomness and ambiguity of the field test to cloud the study. The following sections discuss the behavior of the rover on irregular surfaces, and the schemes for modeling this behavior via the dynamic test platform.

2.1 Rover Behavior - Static Attitudes

The rover on real-world terrain may at any given time and for any of a number of reasons choose to stop and take some stationary scans of its surroundings. Nearly always, its attitude will vary measurably from a planetary reference frame, limited by the rover's slope stability. A controllable platform that purports to emulate rover behavior should then be positionable at pitch and roll angles* up to the stability limits of the rover it models (see Fig. 2.1).

Rover theoretical stability limits are determined from its

*Pitch and roll are defined by the rover configuration. Pitch is rotation about a transverse axis, and roll, about a longitudinal axis.

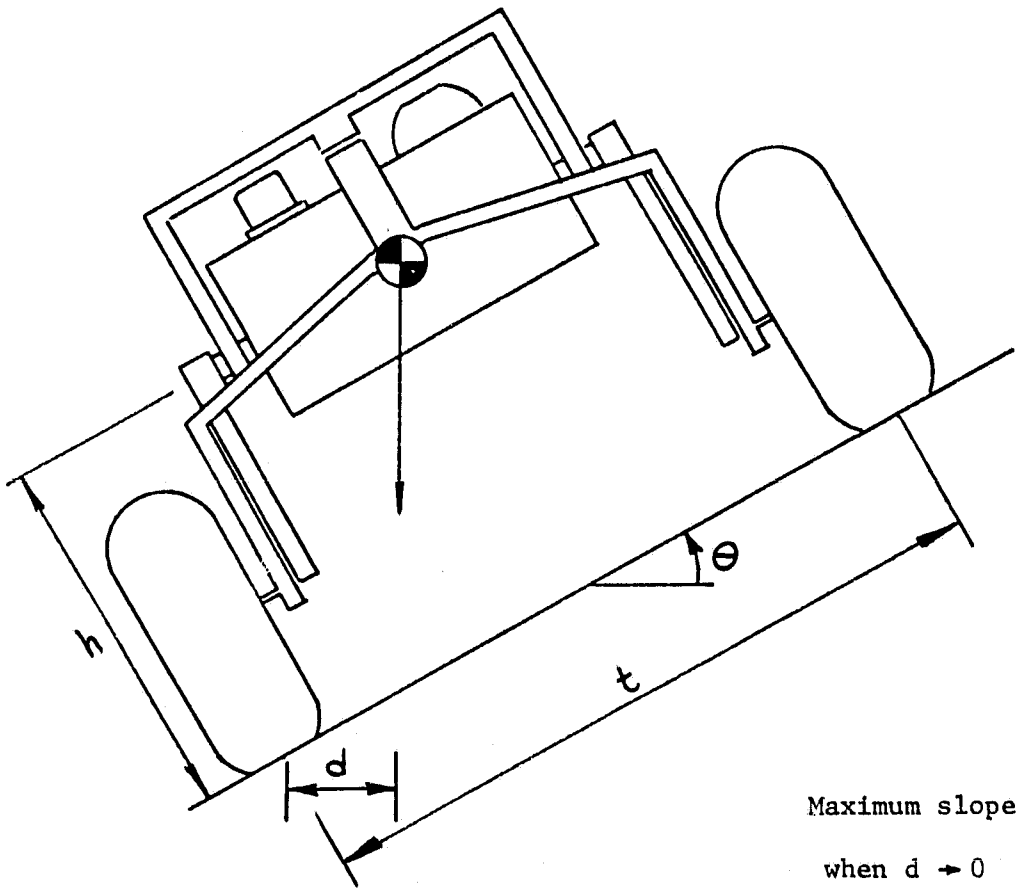

Maximum slope θ

when $d \to 0$

i.e., $\theta = \tan^{-1}(\frac{h}{t/2}) = 43^{o}$

Fig. 2.1
Determination of rover
slope stability limits

wheelbase and track dimensions, and the location of its center of mass. For the RPI rover, this gives a theoretical cross-path stability limit of approximately 43°. (A quirk of the rover design, however, reduces this figure by over 40%, to 25° in certain situations.) This exceeds slopes allowed by the obstacle avoidance algorithms, and any practical situation which might arise, allowing partly to the low shearing strength and traction of the typical soils encountered.

2.2 Rover Behavior - Dynamic Motion

While roving, the wheels of the vehicle travel alternately up and down over all manner of rubble, boulders, holes, etc., up to that size determined to be a hazard. The perturbations experienced by the rover (and the vision system) due to this wheel motion are dependent on the vehicle dimensions, stiffness characteristics, roving speed, and of course bump size. The dynamic test platform is required to simulate these motions as well as the static attitudes outlined previously. In determining what motions are admissible, the lower limit is assigned a value which is typical of small rubble and may be considered as perceivable to the rover. The upper constraint on size is obviously the hazard threshold size. Between these extremes, any combination of disturbances may occur at any wheel, giving an infinity of perturbation modes to which the elevation scanner might be subjected.

In the modeling of rover dynamic behavior, random motion would be a complicated and expensive goal to obtain, and of questionable value as well. For this simulation, periodic motion offers advantages in predictability as well as relative simplicity of design. A range of

appropriate frequencies must be determined for the periodic motions.

Since smaller perturbations are likely to be higher frequency than larger ones, the lower limit on bump size is used to derive the upper limit on frequency. Lower frequencies represent more gentle rover motions, and approach steady-state conditions.

2.3 Emulating Rover Behavior

In developing the test platform concept into machinery, all rover motion is represented by appropriate rotations about pitch and roll axes. In pitch, a front wheel bump results in a rotation about the rear wheels, and conversely. Combinations of front and rear wheel bump motions result in some equivalent rotation. An average situation then may be considered as a rotation about a central transverse axis at ground level. Similar thinking leads to selecting a vehicle longitudinal axis, again at ground level, for rotations in the roll sense.

Working with the intersection point of these two axes, the relative location of the elevation scanner mast is approximated from its tentative position on the rover, as shown in Fig. 2.2. This location is variable in the vertical and longitudinal directions. Allowing this variation via the design of the platform offers the possibility of finding an optimum position for the mast on the rover, this to be determined by the scanner's performance during testing. Changes in mast position might also be seen as representing vehicle dimensional modifications, or motions other than the "mean bump" used in determination of pitch and roll axes.

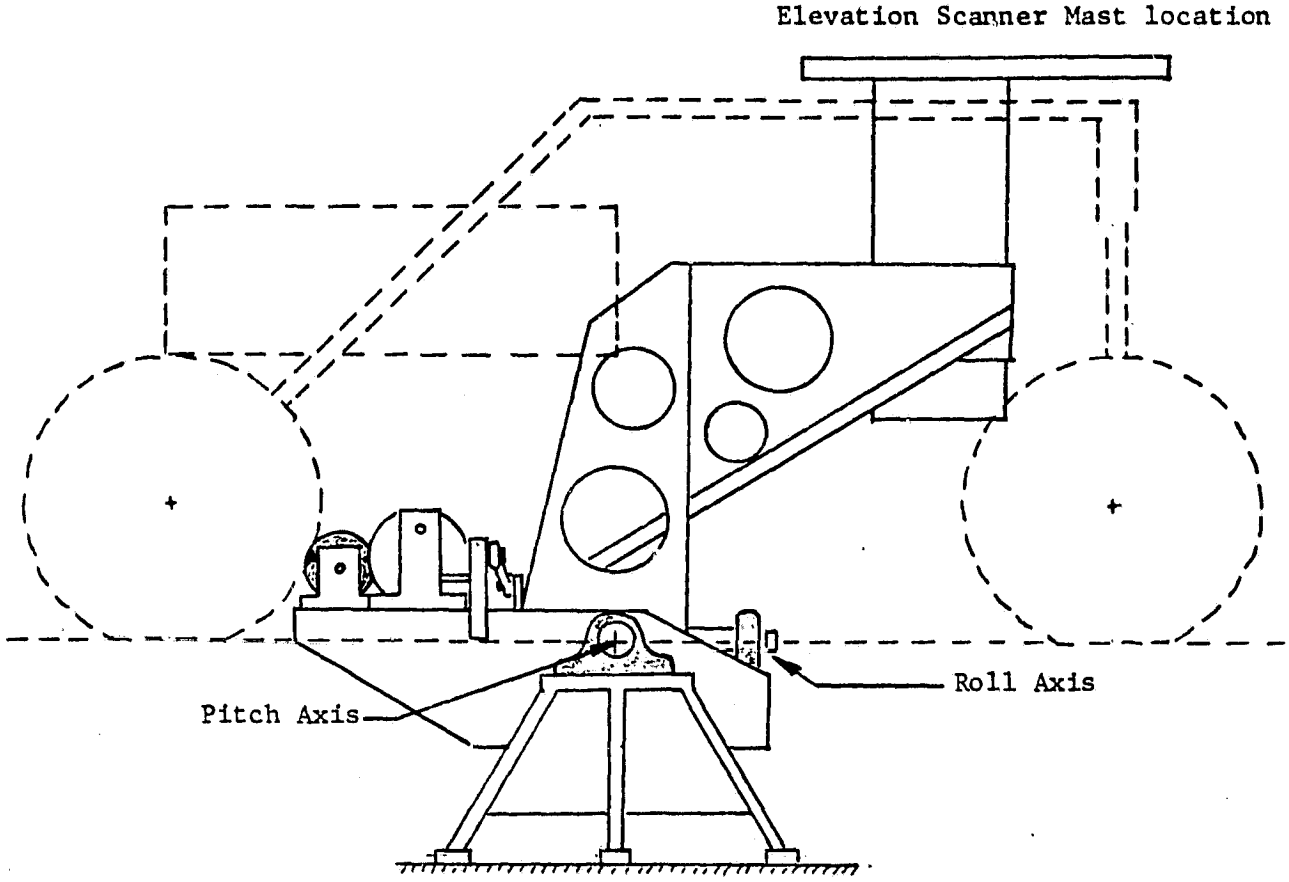

Fig. 2.2
Simulation of rover dimensions

2.4 Determining Motion Parameters

From the rover dimensions, the afore-mentioned theoretical slope stability is approximately 43°. This stability limit also applies to dynamic motions of the rover, that is, the maximum amplitude of periodic oscillation of the platform may be set at approximately 40°. It should be noted that this amplitude limit is valid only if the static angle in the same sense (pitch or roll) is zero. Since the static attitude setting is the mean position about which oscillations occur, it is the sum of the static angle and dynamic amplitude which is limited to 40° or less. This is analogous to the rover traversing a slope and encountering a step with its uphill wheels.

Pitch and roll amplitudes are variable from 0° to 40° in 5° increments. The static setting about which the platform oscillates may be varied between positive and negative 40° in 10° increments, provided the combined displacements are within the previously outlined limits.

Frequency limits are imposed by the perturbations to be considered. The smallest bump of interest is one which first deforms the flexible wheel and further causes disturbance of the rover frame. This bump size is taken to be two inches in height.* To obtain a maximum frequency for this size disturbance, it is noted that the rover's 0.5 m. diameter wheel would contact such a bump through an angle of approximately one radian as it rolls, or a linear distance

*It should also be noted that a combination bump of 2", positive on one side and negative on the other, would result in a rover roll angle of 5°, which is the lower limit on platform amplitude, not coincidentally.

of 0.25 m., one wheel radius. The autonomous speed of the rover is very nearly 0.25 m/s, giving one second travel over the obstacle. Considering this as the positive half of a sine wave, the time for one period becomes two seconds. Thus, the upper limit on bump frequency is taken as 1/2 cps.

Fixing the lower frequency extreme was done less analytically. Desiring a wide range of available, a factor of ten seemed reasonable. Noting that this gives a 20-second period, or in other terms a wheel in contact with an obstacle for 2.5 m. (five times the wheel diameter), this is clearly slow enough that ML/MD performance would not vary significantly from the static case. As an aside, one scan by the ML/MD takes approximately two seconds.

Here it should be noted that we have been working an artificial situation. Although the platform in its oscillating mode will model well the rover's behavior on irregular terrain, the scene scanned by the vision system is not advancing toward the mast. A brief discussion and recommendations concerning this situation are included in Part 4, Concluding Remarks.

2.5 Exploiting the Dynamic Test Platform Concept

In order to make use of the platform's characteristics, a terrain mock-up will be constructed. This mock-up will consist of interesting features of varied size and type, including boulders, slopes, walls and holes. Holes are admissible in the simulation by virtue of the fact that the intersection of the pitch and roll axes of the platform, locating an imaginary ground plane, is in fact some 15

inches above floor level. Certainly holes are valid hazards to the rover. The artificial terrain can be carefully measured to give base data for evaluating the elevation scanner's perception of what it "sees."

With the elevation scanner mast mounted on the platform and the terrain mock-up in front of it, scans may be taken under a wide range of conditions. Some of the experiments will be of the following nature:

1. To determine the quality of the ML/MD's perception of the mock-up, first in a neutral or level attitude.
2. Observe changes in data when a constant static pitch and/or roll angle is introduced. This data change can be compared with analytical predictions.
3. With the platform oscillating, "blurring" of laser returns due to scanner motion can be checked for.
4. The mechanical integrity and stiffness of the mast structure can be verified.
5. Development of the interpretive software
   a. the ability of the interpretive schemes to deal with the fact that azimuth lines are deformed due to changing attitude of the mast;
   b. determination of appropriate data rates;
   c. debugging and refining software;
   d. developing higher levels of sophistication in the software, as for example active and autonomous

modification of data grid density or vision system geometry.

The platform will also serve as a developmental tool for the interpretive algorithms themselves. It will offer an opportunity for some empirical development work as well as simplified testing and verification.

2.6 Optimization of Elevation Scanner Variables

By observation of Platform experiment results, it should be possible to evaluate many of the analytically determined parameters governing elevation scanner operation. Listed here are some items deserving special attention:

1. Position of mast on the rover.
2. Position of major scanner components (e.g., octagonal mirror, detector unit) on mast structure.
3. Laser and detector optics.
4. Mechanical integrity of mast structure.
5. Operational parameters, including scan speed, data grid size and density, theories on voting detector elements, laser beam collimation, detector field of view.

Attention paid these areas during platform experimentation will yield valuable quantitative information. This can help eliminate elusive shortcomings in ML/MD performance before undertaking autonomous roving experiments.

PART 3

PLATFORM DESIGN

3.1 Description

The dynamic test platform is a special-purpose machine, designed to achieve all the goals outlined in Part 2. The platform, shown in Fig. 3.1 and Fig. 3.2, is a large, oscillating machine. Its principal dimensions, between the rotational axes and the elevation scanner location, are equivalent to those of the rover it emulates. A rigid structure, adjustable in two directions, connects the mast to the axes. This structure, the main roll assembly, carries the roll journals which run in pillow block bearings attached to the pitch frame. The pitch frame is another large, rigid structure which includes the pitch journals. These journals run in a second, larger set of pillow blocks, anchored directly to the laboratory floor.

The roll drive system, consisting of motor, transmission and driving mechanism, is supported in the pitch frame. Thus it is stationary in the roll sense, and forces the main roll assembly through its oscillations relative to the pitch frame. The pitch drive system, comprising the same major components as the roll, is mounted separately on the lab floor. Having no motion of its own either in the pitch or roll sense, it is able to force the entire platform in pitching oscillations.

There are three distinct areas of design involved in the platform, each with its own requirements and constraints. The areas into which the different design tasks most readily fit are structural, driving

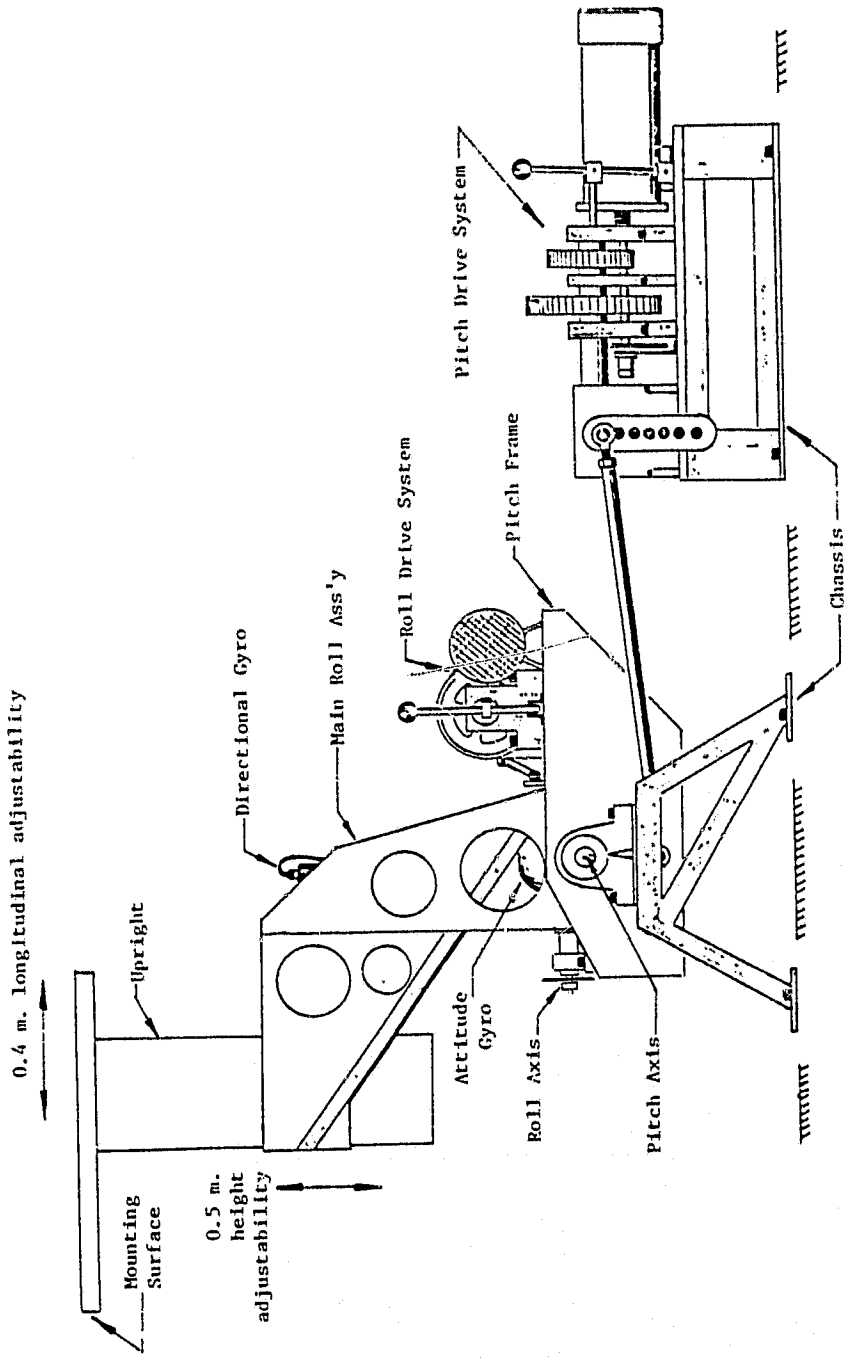

Fig. 3.1
The Dynamic Test Platform

MAST MOUNTED ON THE DYNAMIC TEST PLATFORM

Fig. 3.2

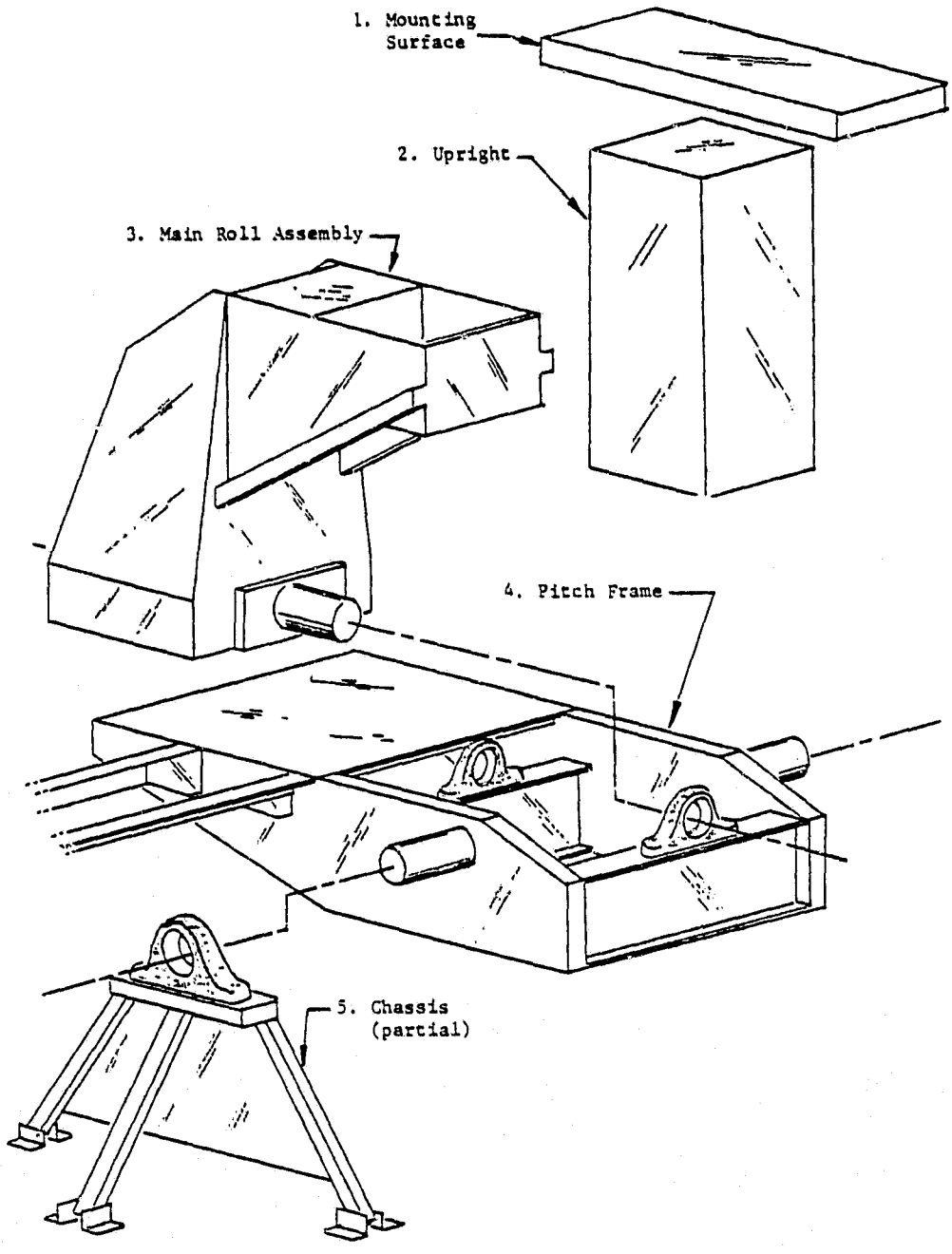

Fig. 3.3

Five Basic Subassemblies

mechanisms, and motors/transmissions. Each of these is here discussed in its turn. More detailed information on the design of all the components may be found in the Appendices, A, B and C.

3.2 Structural

A number of overriding considerations had to be borne in mind throughout the entire platform structural design. These are enumerated below.

1. Rigidity. Angular position of the platform is monitored in pitch and roll by a two-axis gyro and two potentiometers mounted at the rotational axes. To ensure that the attitude of the elevation scanner agrees with that recorded by these instruments at the axes, rigidity is essential between the axes and the scanner location.
2. Oscillating mass. Due to the oscillatory motion of the device, there is obvious benefit in keeping the structural mass low. This keeps forces low in the mounting surface, and for this reason is designed to have high stiffness in bending and in torsion. It is a narrow box in section, narrow in side elevation, and wide in plan. Longitudinal adjustment of mast position on the platform is made by altering the position of this subassembly relative to the next, the upright.
3. Upright. The principle function of the upright is to

facilitate adjustment of mast position in the vertical direction. It is a simple large section box, closed at the top and open at the bottom. Due to the large cross section, torsional stiffness is inherently high. This is very important, due to the form of the loading on the upright. Adjustability is accomplished by alternate mounting positions between the upright and the main roll assembly.

4. Main Roll Assembly. Purely a locating and load-bearing element without moving or adjusting components, this subassembly is a large one. It locates the roll journals and driven (rocker) link of the roll driving mechanism at its lower end, and the upright at its top. An attitude gyro is also located by this element, with its gimbals centered at the intersection of the platform's pitch and roll axes.

5. Pitch Frame. The most involved of the major subassemblies, this carries the roll pillow blocks and, perpendicular to them in the same horizontal plane (horizontal only when the pitch angle is zero), the pitch journals. The pitch frame is made up of two transverse built-up I-sections, two large longitudinal thin-wall box section side panels, three transverse angle extrusions at the rear, and stressed panels on three surfaces. The three angles on the rear of the pitch frame also serve as mountings for the roll motor and transmission assembly.

6. Chassis. Actually a collection of three individual components, the chassis is the item which ties the entire platform to the laboratory floor. It amounts to two paneled tripods to support the pitch pillow blocks, and the pitch transmission frame. The latter is built up of angle section and paneling. It need carry only the weight of the pitch drive system and the reaction force of oscillating the platform in pitch.

3.3 Driving Linkages

The driving linkages take the continuous rotation of the pitch and roll motors as inputs and produce near-sinusoidal periodic oscillations as outputs. Governing parameters are the desired variable mean output angles and amplitudes of oscillation. As usual, simplicity and expense of fabrication were of high priority in the linkage design.

The linkages are classed as four-bar crank/rockers. Required adjustments are made by alternate locations of the ends of the coupler links. Moving the end on the crank link changes the effective radius of the crank, and hence the amplitude of the output oscillation. Available variations are 0° to 40°, by 5° increments. Moving the opposite end of the coupler, the rocker end, changes the static (or mean) angle of the platform. This is due to the design of the rocker link. It is a heavy plate in both the pitch and the roll systems, with nine locating points for the coupler. These points are along an arc of constant radius, arranged in 10° increments about the vertical from -40° to +40°. By

choosing an alternate position for this end of the coupler link, the linkage proportions are unaffected but the angle between the oscillating assembly and its rocker "link" (the line between the rocker pivot and the coupler link attachment) changes. In this way a static or mean angle for the platform may be introduced, and any oscillations are about this new average angle.

In order to meet the operational goals for the platform, certain linkage proportions must be adhered to. Nearly sinusoidal output motion, though not essential, is desirable. This form of oscillation would aid in predicting and post-processing elevation scanner data. It is essential, however, that the platform be capable of $\pm 40°$ angular motion without the driving linkage locking.

In order to obtain oscillations approximating sinusoidal, reference is made to Fig. 3.4, and the following relations:

$$R = b(\sin\theta_o)$$

$$\text{or } \theta_o = \sin^{-1}(R/b)$$

where R = crank radius

b = rocker length

θ_o = output angle amplitude.

From this expression a crank radius is found for each desired output amplitude. This is only an approximation, since a four-bar does not generate a true sinusoid due to the angularity of the coupler. Sine generators were considered for use, but the increased fabrication expense was deemed unacceptable for the marginal improve-

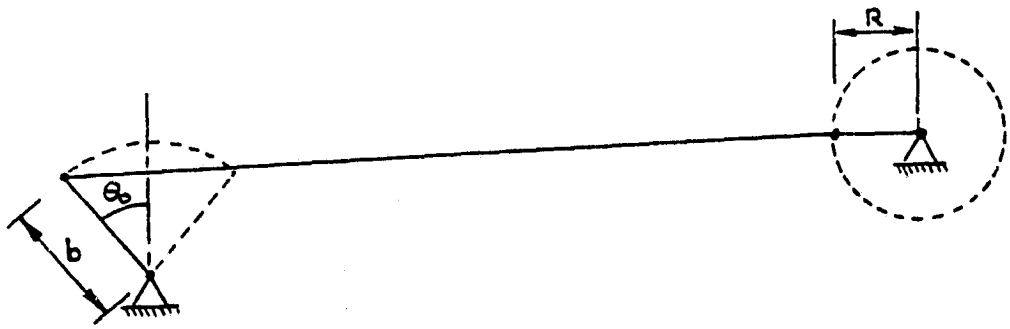

Fig. 3.4

Platform Driving Linkages

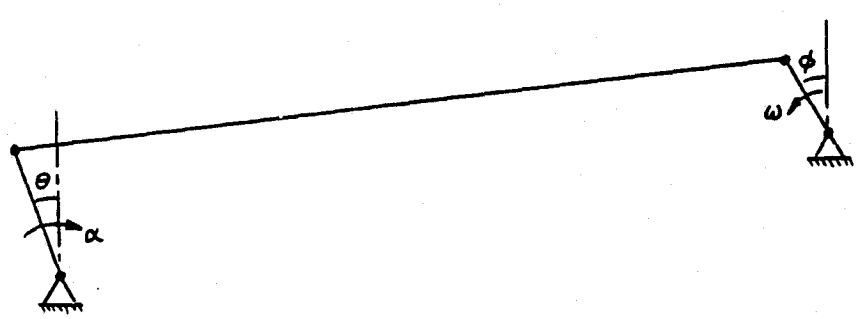

ment in predictability of output. The approximation by this four-bar is quite good provided the coupler is sufficiently long. Rocker lengths were determined based on compressive loads in coupler links and practical considerations such as rod end bearing size. Given a rocker length, the above relationship is used to derive a crank radius for each output amplitude angle.

Determining torques and forces through the driving linkages requires construction of two mathematical models of the platform, one for pitch and one for roll. Using a worst-case situation in which the platform is operating at maximum amplitude and frequency (limits determined in Part 2), with the mast positioned as far from the rotational as the built-in adjustability will permit, the rocker torques are estimated. This is done by representing the scanner mast, the various platform subassemblies, and other major masses as concentrated masses at specified locations. A simple torque balance is calculated for the extreme angular positions, where masses are displaced to their limits, and accelerations are at their maxima. These maximum accelerations are determined by differentiation of the earlier relation for output angle:

$$\theta_o = \sin^{-1}(R/b)$$

Expressing this equation in time-varying form:

$$\theta(t) = \sin^{-1}(R/b)\sin(\phi)$$

$$\phi(t) = \omega \cdot t$$

where $\theta(t)$ = inst. output angle ω = frequency

$\phi(t)$ = inst. crank angle t = time

Differentiating $\theta(t)$ twice with respect to time:

$$\alpha(t) = \frac{d^2\theta}{dt^2} = \omega^2 \sin^{-1}(R/b)\sin(\omega t)$$

The magnitude of this acceleration is a maximum when ω is maximum (0.5 cps. or π rad/s), and $\phi = \omega t = \pi/2$.

The expression for the maximum acceleration becomes:

$$\alpha_{max} = \pi^2 \sin^{-1}(R/b)\sin(\pi/2)$$

Recalling the original expression giving the value of (R/b) for the maximum angular displacement, $\theta_o = 40°$, the magnitude of the maximum angular acceleration is:

$$\alpha_{max} = 6.89 \text{ rad/s}^2$$

Further development of these acceleration and torque expressions can be found in Appendix B. Included there is an explanation of the method used in determining the location of the roll drive components' major masses relative to the pitch axis. Effective choice of this location can have a beneficial influence on the magnitude of the pitch rocker torques.

Having a value for the maximum torques required at the rocker, the corresponding torque must be determined at the crank link. Recourse is made to the concept of instantaneous centers of rotation, illustrated in Fig. 3.5. Using this technique, the crank torque can be found as a function of the instantaneous geometry of the mechanism and the value of the rocker torque. This process is repeated for input (crank) angles of 0° to 360°. The plotted results form a torque profile, giving crank torque vs. crank angle. By noting the rotational speed of the crank

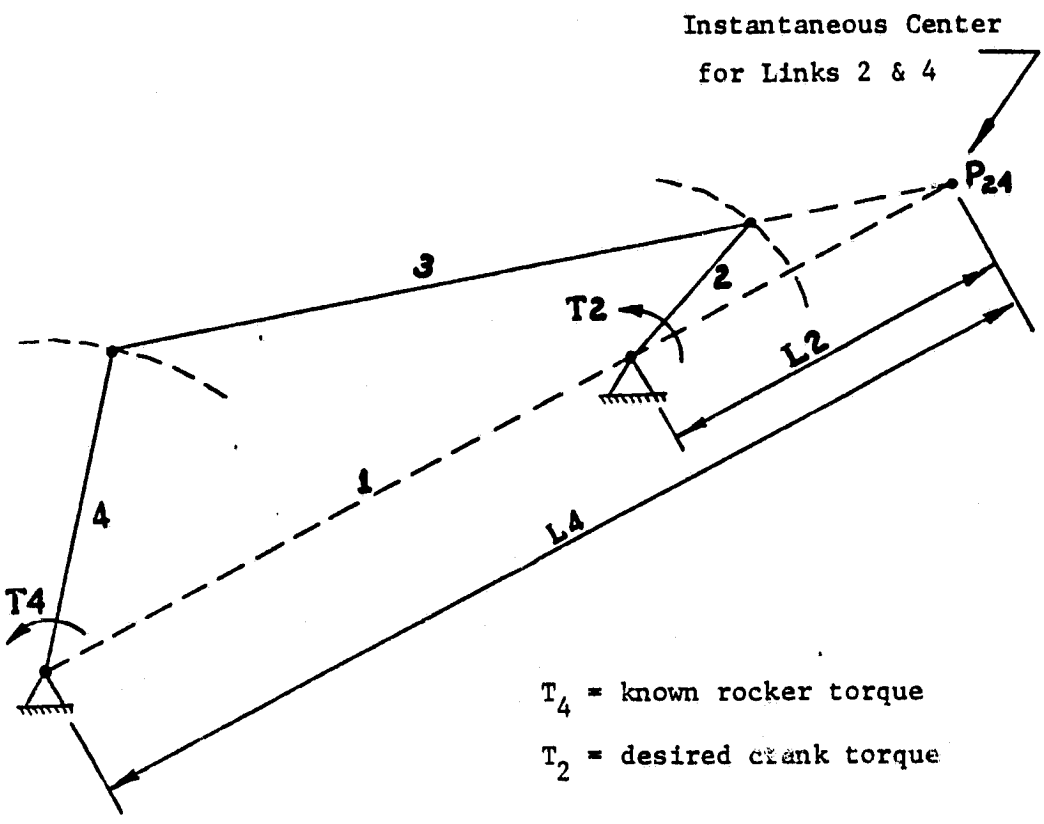

T_4 = known rocker torque

T_2 = desired crank torque

$$\frac{T_2}{L_2} = \frac{T_4}{L_4}$$

Fig. 3.5

Instantaneous Centers of Rotation

it is easy to add a horsepower scale on the abscissa of the profile. This makes a very convenient device to aid in the selection of motors.

The nature of the platform's motion is such that the torque (or power) profiles are characterized by steep peaks and deep valleys, averaging to a small absolute value. This indicated that a drive system comprising a small, low-power motor supplemented by a high-capacity flywheel for energy storage during the valleys of the profile might be called for. Study showed, however, that the inertia of a flywheel which could supply enough energy for the peaks when a small (1/8 hp range) motor is used was prohibitively large. It proved more satisfactory to select motors with adequate reserve power for the peaks. The flywheel question is duscussed in greater depth in Appendix C.

3.4 Motor and Transmissions

Through the design of the driving mechanisms, acceptable power ranges for the pitch and roll motors are derived. Another question in motor selection was the width of the operating speed range. In Part 2, a guideline of 10:1 speed variation was set. No motors were available with a useful range approaching this. The widest obtainable (the motors eventually chosen) was from 500 to 1800 rpm, a factor of 3.6. Two different gear ratios would be required to realize the desired range. The difference between these two ratios was chosen as 3:1, resulting in an overall operating speed range of 10.8:1. This makes the limited range motors wholly acceptable. They are permanent magnet dc type, manufactured by Dayton. The pitch motor is 1-hp, the roll, 1/2-hp. Data may be found in Appendix C.

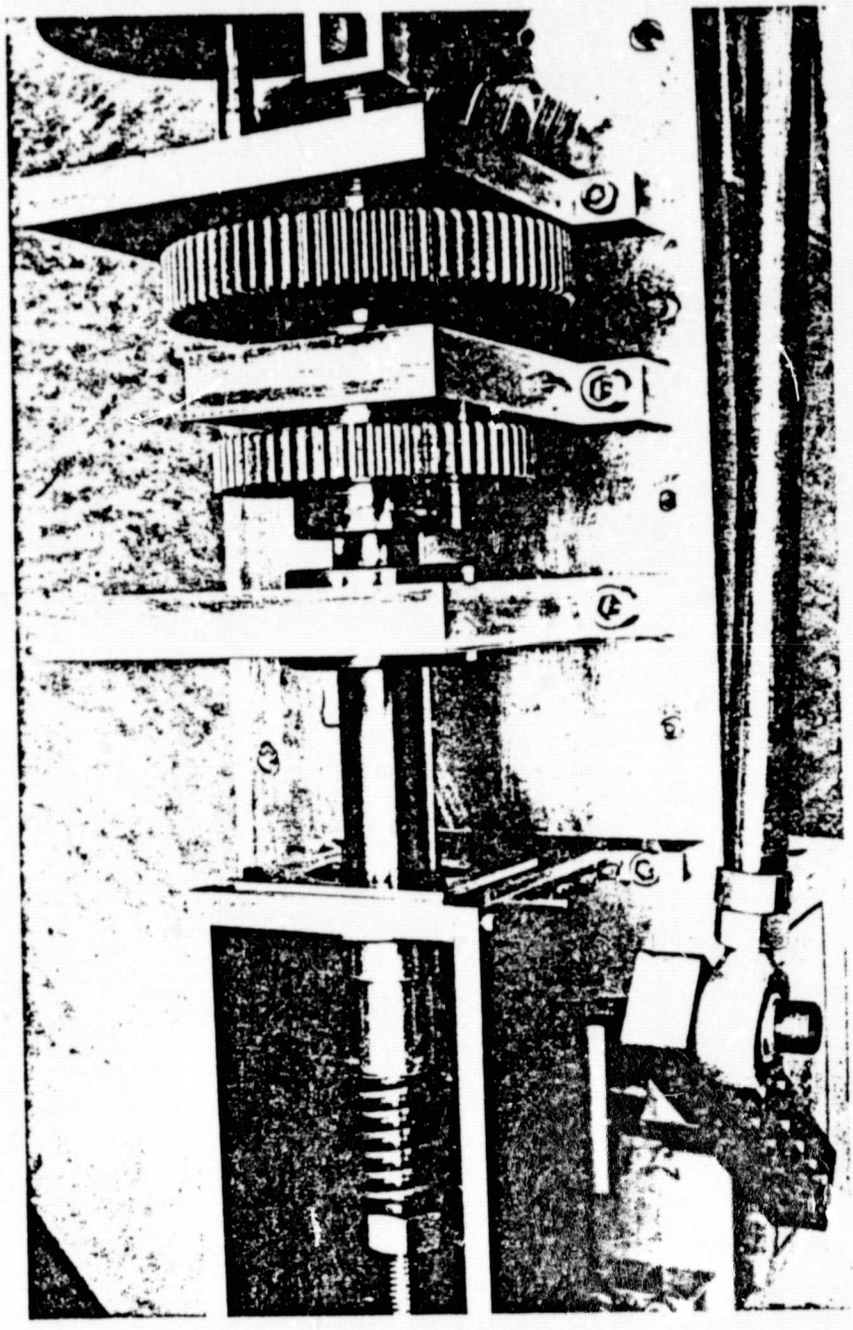

Fig. 3.6. Pitch Transmission.

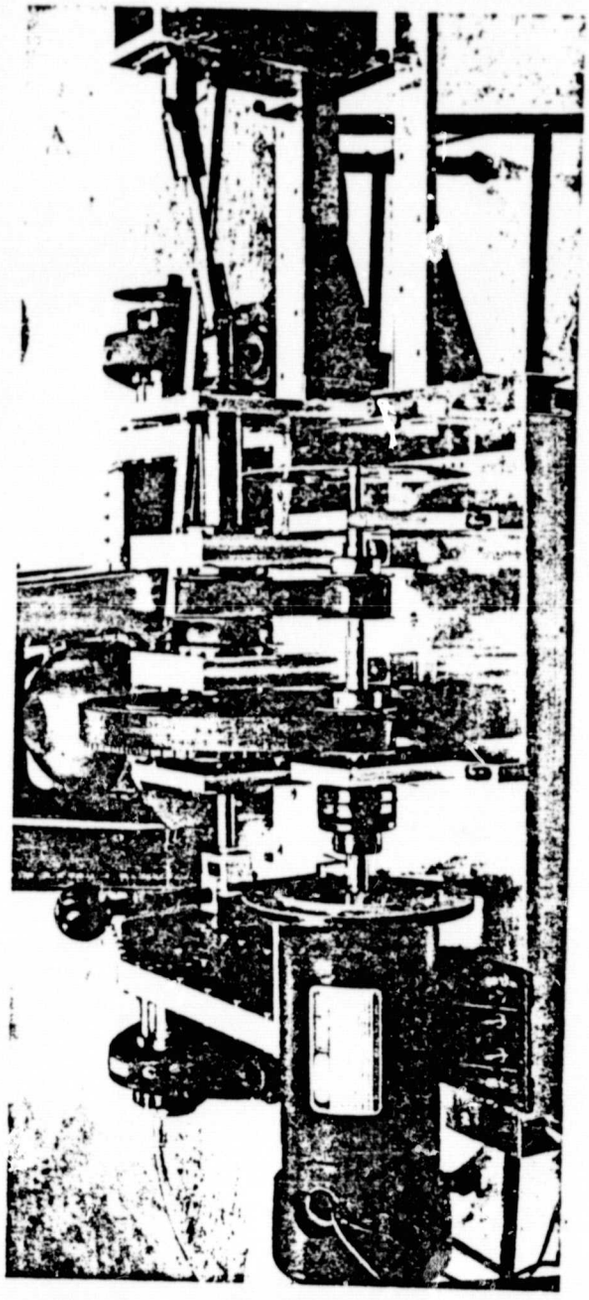

Fig. 3.7. Roll Transmission

With the dual-range requirement, the simple matter of selecting suitable gear reduction for the motors had grown to one of designing a pair of two-speed transmissions. Ratios were already defined. A maximum motor speed of 1800 rpm and a required crank speed of 0.5 cps or 30 rpm meant a high ratio of 60:1. The factor of 3 difference in ranges gives a low range ratio of 180:1. It then became a process of designing and selecting the appropriate hardware.

With such large required reductions, a logical starting point was worm gearing as a final transmission ratio. Another benefit of worm gearing, aside from high available ratios, is its non-reversing characteristic. The crank link is driven directly off the worm gear. It is then impossible for the platform to reverse the driving forces, that is, the driven link cannot become the driver. The platform is constrained in position by the worm, and no braking device is required for static testing.

Strength, size and considerations of available primary reduction ratios, covered in Appendix C, led to selecting ratios of 40:1 for roll and 30:1 for pitch. The primary ratios then become 4.5:1 and 1.5:1 in roll, 6:1 and 2:1 in pitch.

The dynamic test platform was designed fast-track, that is, while one piece of hardware was being fabricated, others were still in various design phases. The roll transmission was designed before the pitch, as its elements constitute a portion of the structure of the platform itself (the pitch frame). In the interest of light weight, reduced maintenance and predicted ease of alignment, a set of gearbelts and pulleys were selected for primary reduction. It was later found

that the torque requirements in pitch could not be handled by gearbelts of practical size. Spur gears were used in their stead. The experience of fabricating and struggling with the various components necessitated by the gearbelts (partly to allow the required center distance adjustment) has led to the hindsighted observation that spur gearing would have been a more satisfactory choice in roll as well. Details of component selection may be found in Appendix C.

With two ratios in each transmission, a gearchange mechanism was needed. The requirements to be met were adequate strength, ease of operation, and again, ease of fabrication in the interest of cost. A desirable feature would be constant meshing of the drive elements, as changing pieces of hardware to change ratios would certainly detract from the ease of operation.

A mechanism was devised to meet these criteria. The principle ingredient is the dog shaft. This shaft has two square sections (dogs) designed to mesh with internal squares within the hubs which carry the gears (gearbelt pulleys in the case of the roll transmission). There is one such hub for each gearset, and a third acting as an output hub, connecting the transmission with the worm reducer set. The longer of the dogs is constantly engaged with the output hub (see Fig. 3.8). The smaller dog can be moved between the hubs of the two adjacent gears, selectively engaging one ratio or the other. It should be noted that the internal square sections in the gear hubs are separated by a distance greater than the width of the selecting dog, eliminating the chance of engaging both ratios simultaneously. This device gives easy, reliable gearchange with a minimum of extraneous hardware.

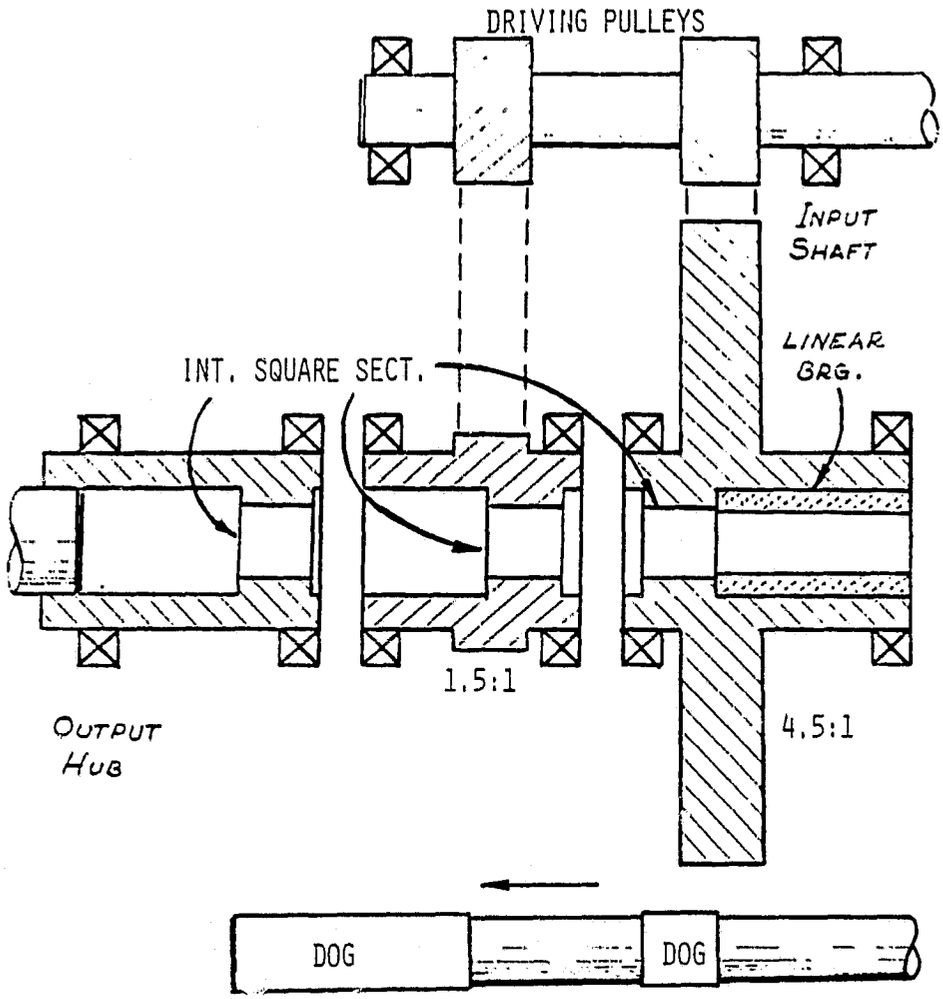

Fig. 3.8

Roll Transmission Schematic

Pitch transmission is similar,
but uses spur gearing rather than gearbelts

Motor speed is feedback-controlled by small tachometers running at motor speed. A digital readout is supplied by virtue of slotted disk optical encoders mounted with the tachs.

Sending attitude information are potentiometers for pitch and roll, as well as the rover's attitude gyro. This redundancy is intentional, as the gyro characteristics are to be studied during tests. This is done to improve vehicle state data accuracy in later autonomous roving experiments. Calibration of the pots and gyro is achieved with dial gages located, along with the potentiometers, on the pitch and roll axes of rotation. Although it gives no information useful to elevation scanner data interpreters, the rover directional gyro is also mounted, so that its behavior may be studied to the benefit of future work.

PART 4

CONCLUDING REMARKS

4.1 Remarks

In the foregoing text, the theory and design procedures behind the dynamic test platform have been discussed. Some qualifying remarks are called for here.

The objective of this device is not to replace the rover. It is, rather, intended to be a versatile diagnostic tool. As such, it has limitations. Principle of these limitations is the fact that all rover motion is reduced to the case of sinusoidal oscillations about constant axes. Although this factor reduces the type of motions the elevation scanner may be subjected to, it affords several advantages. Among these are reduced mechanical complexity, repeatability and predictability of motion.

Another limitation, mentioned in Section 2.4, is that the test platform does not allow within its concept for the approach of the terrain relative to the rover (or the elevation scanner, more specifically). The platform is fixed to the laboratory floor. For full development of rover modeling schemes, a moving terrain mock-up could be constructed. It could be made to advance toward the platform during the test, as if the platform (and hence the scanner) were moving forward over the terrain. This task is left for the future.

4.2 Assembly and Verification

Lessons are inevitably learned during the assembly and verification phase. As mentioned in Section 3.4, the difficulties asso-

ciated with gearbelt power transmission were such lessons. Spur gearing would have been the better choice for the roll transmission as well as the pitch.

Another area of concern which did not surface until the assembly and verification phase of the program was the transverse rigidity of the pitch frame (refer to Appendix A, Fig. A.7). The reaction to the roll driving torque is a rather large transverse force on the back portion of the pitch frame. This situation required extra gusseting in the horizontal plane to more rigidly tie the rear deck and side panels together. An alternative design of the rear deck would have obviated this patchwork.

4.3 Summary

At this writing, the dynamic test platform is mechanically complete, and the electronic controls are nearly ready. At the present, it is therefore impossible to assess the overall performance and value of the platform. It is projected that the platform will serve at length to aid testing and refining the hardware and software of the ML/MD system. It is likely that a great deal of time will be devoted to static testing on the platform. This situation must be thoroughly studied and understood before dynamic testing is practical. When development reaches a stage such that the performance of the ML/MD system is fully understood, attempts may be made at optimizing its hazard detection abilities.

For all these experiments, the dynamic test platform should prove an invaluable tool. Parameters of the experiments can not only

be quantified, but maintained for long periods if necessary, and precisely repeated or subtly modified for series of successive tests. Clearly, these cannot happen under autonomous roving conditions. Without such quantitative, controlled testing and development, field testing on the rover would be a long, arduous task, and valuable results would be much slower in coming.

APPENDIX A

STRUCTURAL DEGIGN

Contained within this appendix are some of the design details of structural components. Covered are the five major subassemblies:

1. Mounting surface.
2. Upright.
3. Main roll assembly.
4. Pitch frame.
5. Chassis.

Descriptions, assembly drawings and loading diagrams are included.

A.1 Mounting Surface

The mounting surface serves to locate and attach the elevation scanner mast to the platform. It also facilitates alternative positioning of the mast in the longitudinal direction (in terms of rover orientation). Total longitudinal adjustment range is 0.4 m. in 0.1 m. increments.

The shape of the mast and loading of the mounting surface (due to the presence of the mast) lead to a long, narrow box section design (see the assembly drawing, Fig. A.1). Assuming the upright and all other structures below the mounting surface to be rigid, the loading on the mounting surface is as shown in Fig. A.2.

Cantilever bending in two directions and twist about a longitudinal axis of symmetry are to be minimized, with minimal weight. For all design purposes, it is assumed that the platform moves at 40°

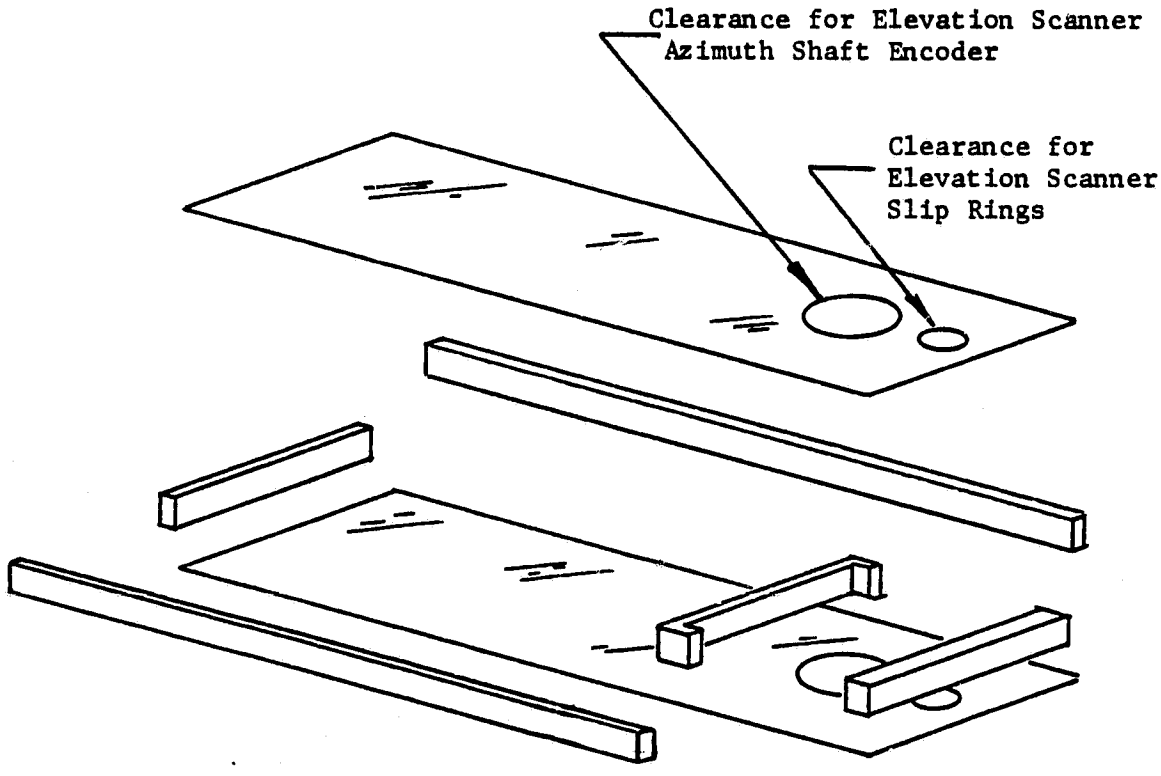

Fig. A.1
Mounting Surface

Assembly drawing

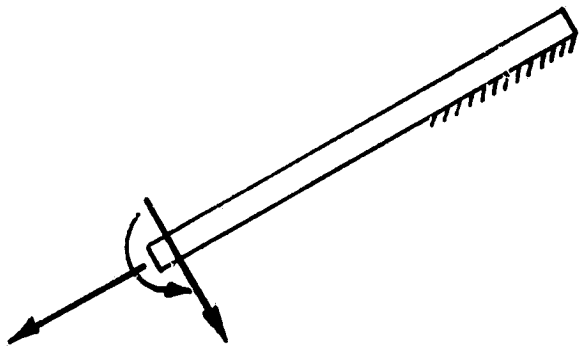

Mast pitch reaction

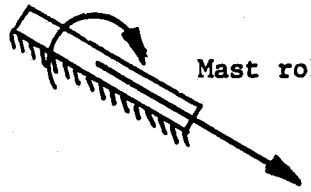

Mast roll reaction

Fig. A.2

Mounting Surface
loading

amplitude and 0.5 cps in both pitch and roll.

The largest bending deflection is in the vertical direction, approximately 0.005 inches. Total longitudinal twist is less than 0.048°. Weight of the mounting surface is 7.25 lbs.

A.2 Upright

The upright carries the mounting surface on its top, and allows vertical adjustment of mast position. Five positions are provided, varying by 0.1 m. each. It is a large open box section (see Fig. A.3, assembly drawing).

Loading on the upright is as shown in Fig. A.4. Axial twist, bending in two directions and tear-out of the mounting surface studs were design criteria. Maximum twist is 0.0005°, with 0.0007 inches transverse deflection. Maximum bending stresses are on the order of a few percent of the material (aluminum) yield strength. Weight of the upright is 11.2 lbs.

A.3 Main Roll Assembly

The main roll assembly is a highly complex structure. It has specific component locating duties, and is subjected to large and numerous loads.

Starting at the bottom end, the main roll assembly must locate the roll journals and rocker link. This points to a highly loaded area of the assembly. The bottom end of the assembly is built up from deep-section aluminum channel and rectangular sections, paneled on top and locating the attitude gyro. An assembly drawing is shown in Fig. A.5

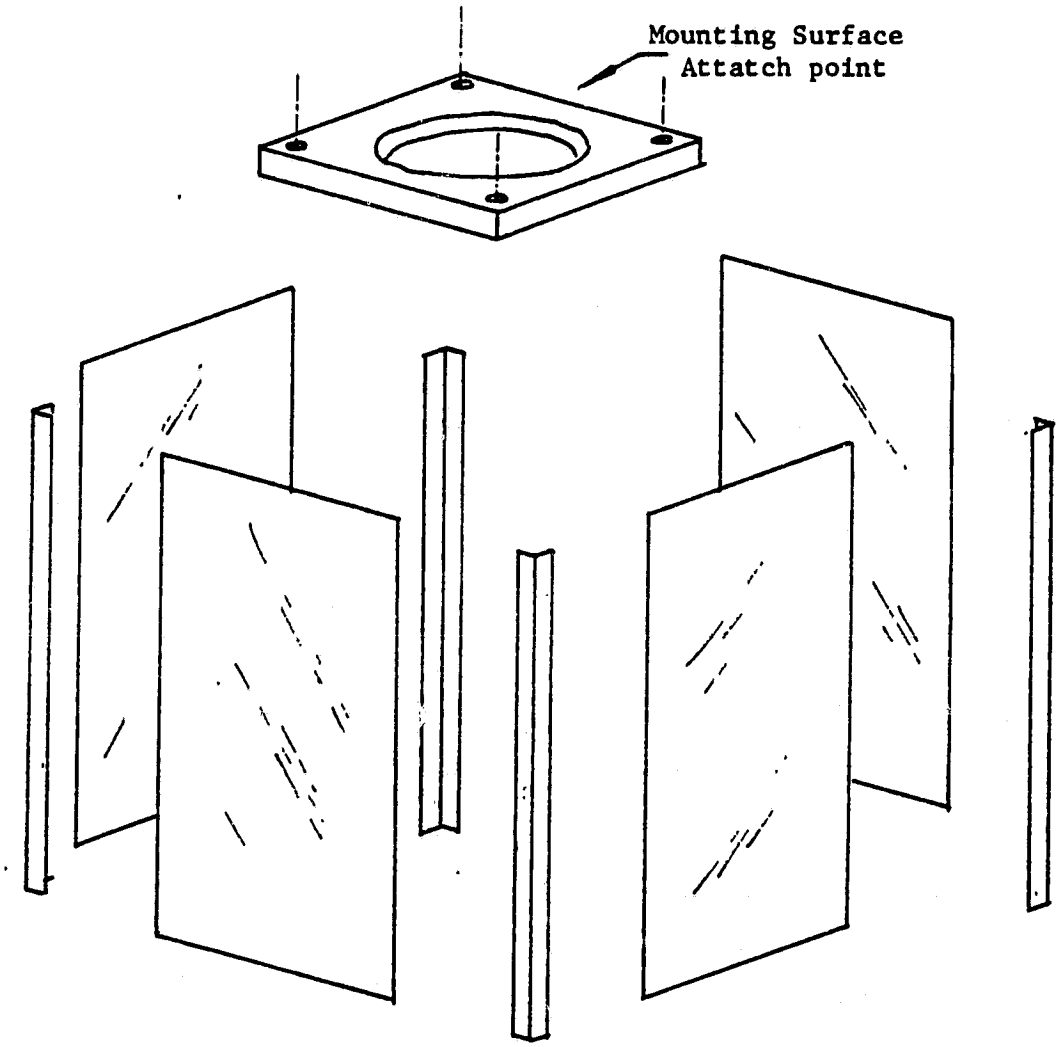

Fig. A.3

Upright

Assembly drawing

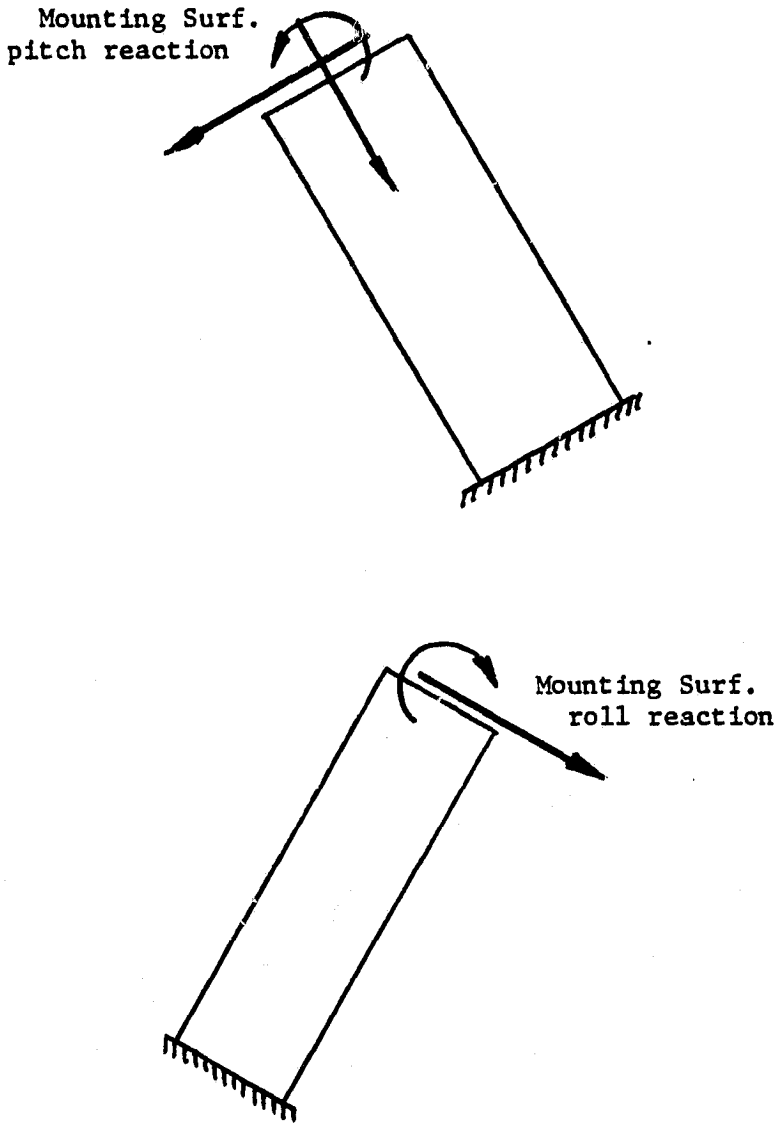

Fig. A.4
Upright loading

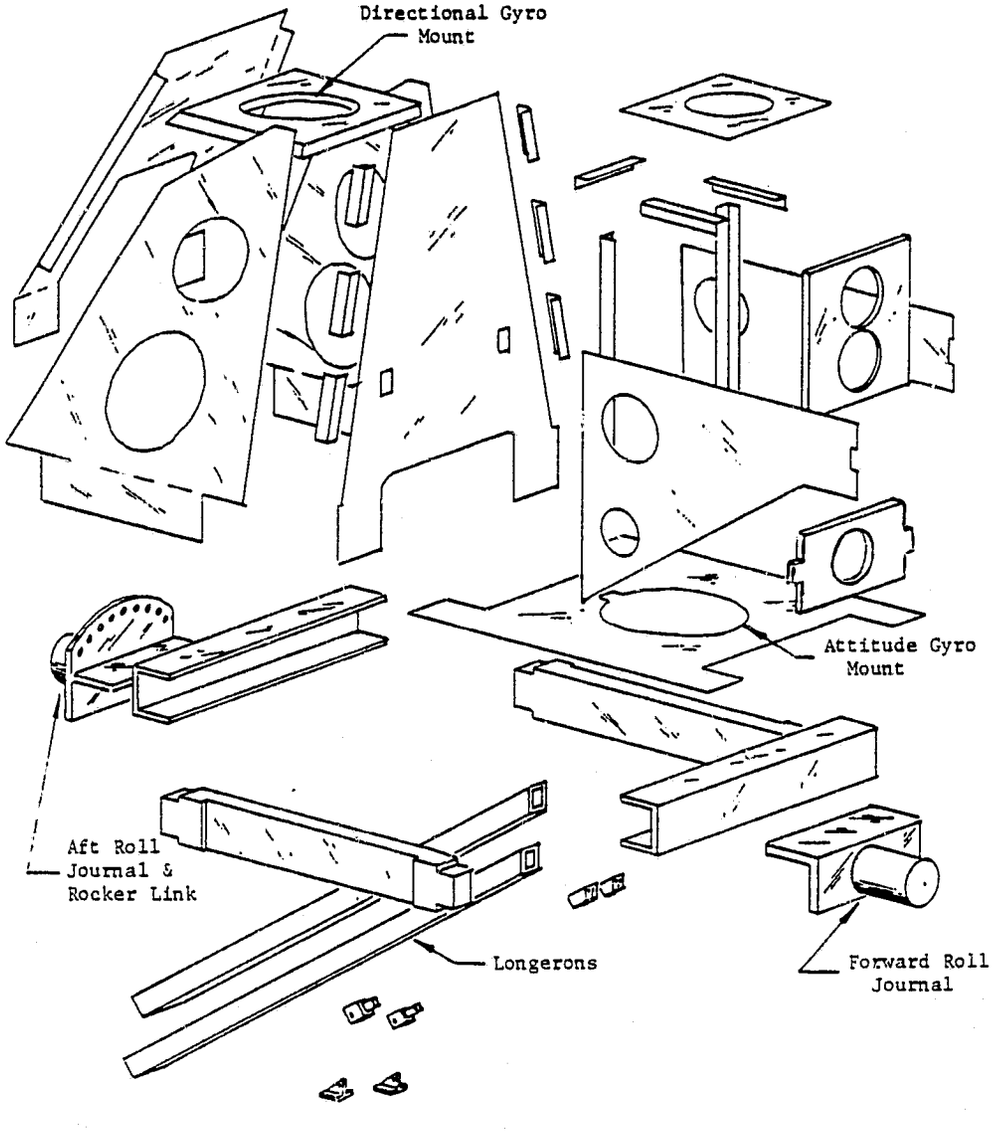

Fig. A.5

Main Roll Assembly

Assembly drawing

and additional perspective can be gained from the subassembly drawing, Fig. 3.3.

Moving to the top end of the main roll structure, the upright must be carried at the most extreme portion of the assembly. A pitching motion develops longitudinal loading (tension) between the upright and the bottom end of the roll assembly. To take out these loads, two square-section aluminum longerons run from the upright location to the channel section at the rear of the bottom.

Extending from the channel sections at the base are the roll journals, large diameter stainless steel stub axles. The flange for the rear of these two journals also forms the rocker link of the roll drive system.

The greater part of the main roll assembly is made up of 1/8 inch aluminum paneling (6061-T6), acting as shear plates. A summary of the loading situation is given in Fig. A.6.

A.4 Pitch Frame

The duties of the pitch frame are as varied and complex as those of the main roll assembly. The pillow blocks in which the roll journals are supported are mounted on built-up I-sections forming front and rear transverse rails of the pitch frame. Perpendicular to these are the pitch journals, pressed into mild steel flanges. The flanges are sandwiched by the faces of the side panels. These built-up box panels are narrow and deep, of high rigidity in the vertical. An assembly drawing of the pitch frame is provided in Fig. A.7.

Behind the location of the main roll assembly, on the rear

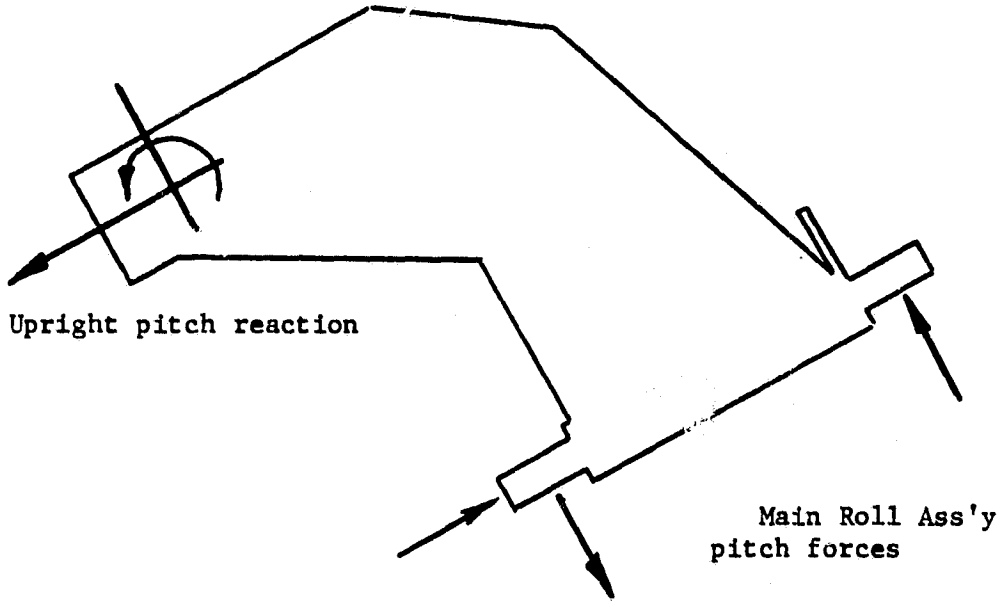

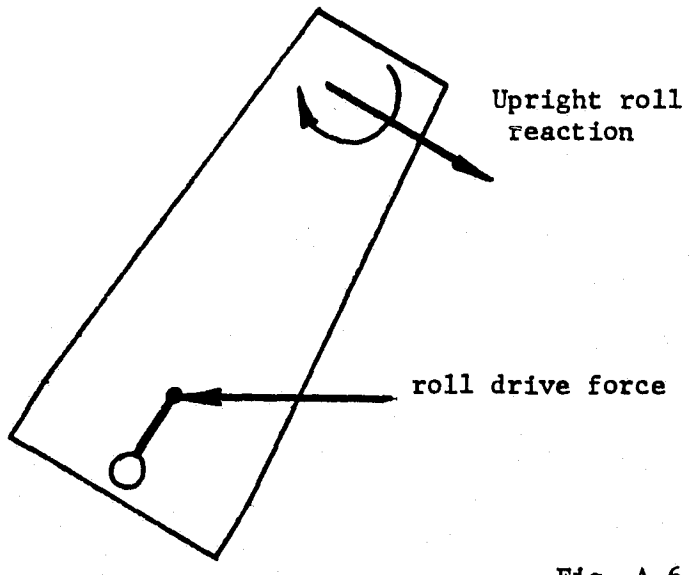

Fig. A.6

Main Roll Ass'y
loading

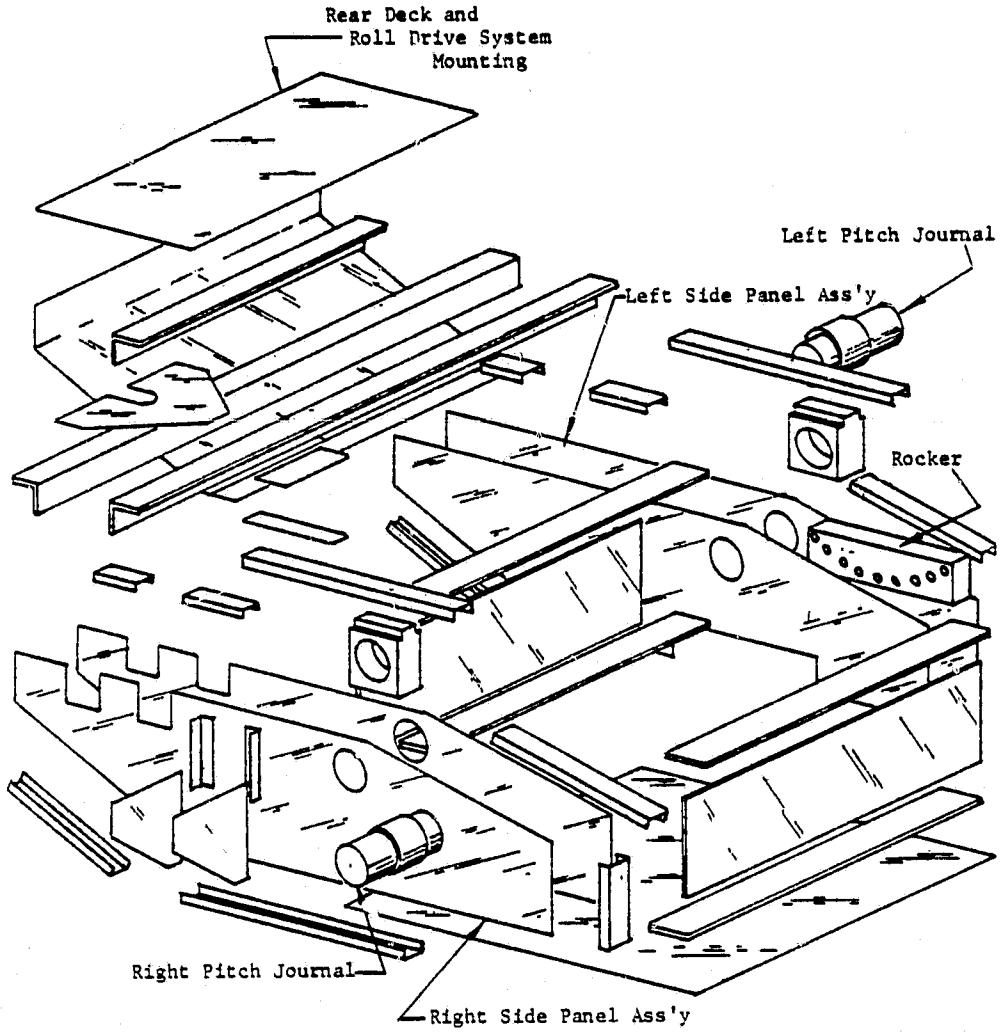

Fig. A.7
Pitch Frame
Assembly drawing

deck of the pitch frame, is the position of the roll drive system. This system is carried on three heavy transverse angles, extensively panaled. The worm reduction set, with the crank link, is mounted on an extension of these angles. As the roll assembly is driven via the worm gear, there are oscillating loads developed parallel to the angle sections. This necessitates horizontal gusseting where the angles tie to the side panels. The deep pitch frame is paneled across the underside to negate twist and resist the loads summarized in Fig. A.8.

A.5 Chassis

The simplest of the subassembly structures, the chassis, actually comprises three structures. Two tripods support the pitch pillow blocks and hence the entire platform. The balance of the chassis is the pitch transmission frame. It is a built-up assembly of aluminum angles and paneling.

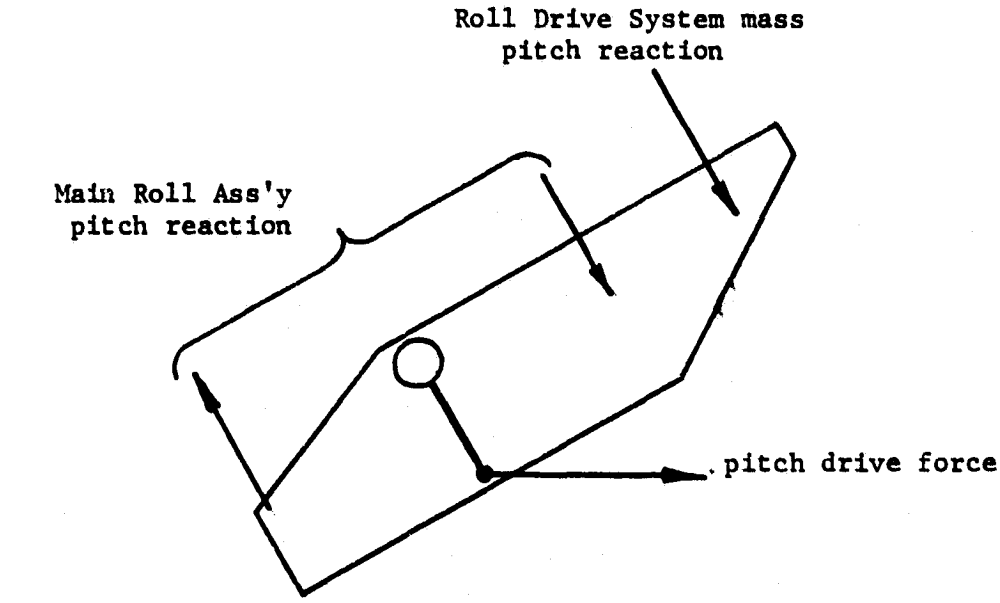

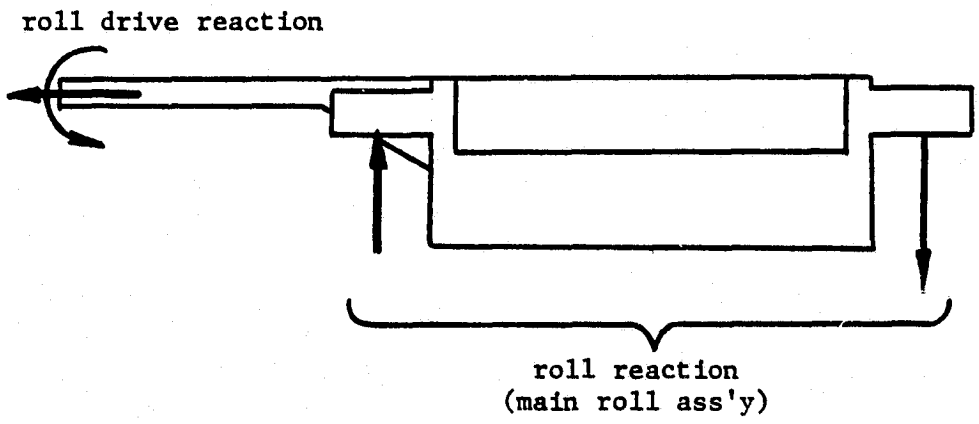

Fig. A.8

Pitch Frame loading

APPENDIX B

DRIVING MECHANISMS

This appendix details the development of the dynamic test platform's driving mechanisms. They are responsible for turning continuous rotation input from the motors into near-sinusoidal oscillation of various amplitudes about various average angular positions.

The form of the driving mechanisms is four-bar crank/rocker. The rocker, or output link, is part of the oscillating platform assembly. Its motion amplitude, as determined in Part 2, varies from 0° to 40° in 5° increments. This is accomplished by altering the crank link effective radius. Given a sufficiently long coupler link, the approximation

$$R = b \sin \theta_o$$

$$\text{or} \qquad \theta_o = \sin^{-1} (R/b) \tag{B.1}$$

is a good one. This relates output amplitude, θ_o, to crank radius R (refer to Fig. B.1). This expression forms the basis for the determination of platform accelerations and the torque and horsepower requirements for the drive motors.

B.1 Platform Acceleration

Expressed in time-varying form, Eq. B.1 becomes

$$\theta(t) = \sin^{-1} (R/b) \sin\omega t \tag{B.2}$$

ω = crank frequency

Differentiating Eq. B.2 twice with respect to time

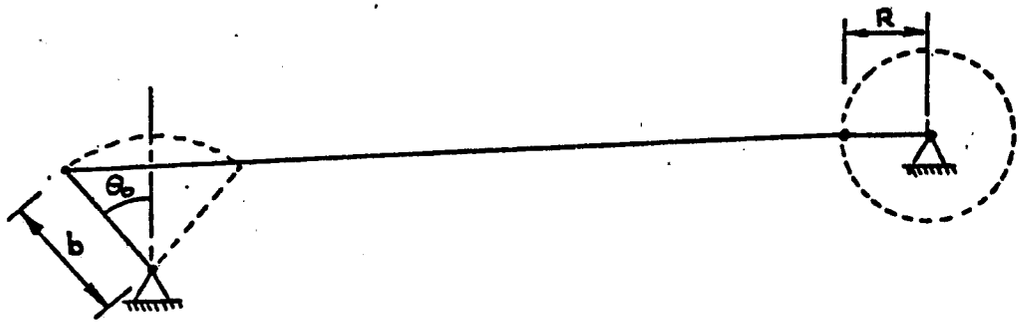

Fig. B.1
Platform Driving Linkages

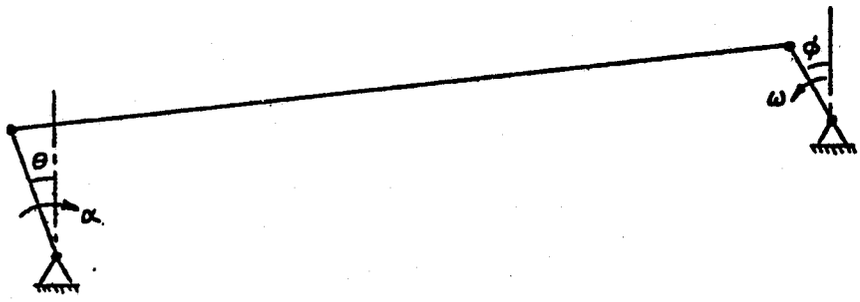

$$(t) = \frac{d^2\theta}{dt^2} = -\omega^2 \sin^{-1}(R/b)\sin\omega t \qquad (B.3)$$

Equation B.3 gives the angular acceleration of the rocker link (hence the appropriate platform assembly) as a function of crank radius (or output amplitude, from Eq. B.1), crank speed and time. For determination of design parameters, 40° amplitude at 0.5 cps (30 rpm) crank speed has been used. Using these values in Eq. B.3 and noting that

$$\sin^{-1}(R/b) = 40° = 0.698 \text{ rad}$$

and $$\omega = 0.5 \text{ cps} = \pi \text{ rad/s}$$

gives $$\alpha(t) = -\pi^2(0.698)\sin\omega t$$

$$= -6.89\sin\omega t \qquad (B.4)$$

the magnitude of which is obviously maximum when $\omega t = \pm \pi/2$. This leads to the maximum value for the angular acceleration of the platform:

$$\alpha_{max} = 6.89 \text{ rad/s}^2 \qquad (B.5)$$

To gain a more complete picture of the development of these accelerations, Eq. B.3 has been used to determine the maximum platform acceleration for a full range of amplitudes and crank speeds. These values are compiled in Table B.1.

This acceleration information is used to determin torques at the rocker and at the crank. From these, horsepower requirements are identified.

output amplitude (deg.)	crank speed			
	3 rpm	10 rpm	20 rpm	30 rpm
5	0.0086	0.0957	0.3829	0.8616
10	0.0172	0.1914	0.7654	1.7222
15	0.0258	0.2871	1.1484	2.5839
20	0.0345	0.3828	1.5313	3.4455
25	0.0431	0.4785	1.9138	4.3061
30	0.0517	0.5742	2.2968	5.1677
35	0.0603	0.6699	2.6797	6.0293
40	0.0689	0.7656	3.0622	6.8890

Table B.1
Platform angular acceleration (rad/s^2)

B.2 Rocker Torques

A model of the platform is developed to show the principal masses and the accelerations they undergo. An example of this is shown in Fig. B.2. Equations of motion, derived from such a model, define the torques required at the rocker link to produce the resulting motion.

From Fig. B.2(b) a torque balance gives

$$T = m_1 s_1^2 \alpha + W_1 s_1 \sin(\theta+\gamma) + m_2 s_2^2 \alpha - W_2 s_2 \cos\theta$$

$$T = W_1 s_1 [s_{1g} \frac{\alpha}{g} + \sin(\theta+\gamma)] + W_2 s_2 [s_{2g} \frac{\alpha}{g} - \cos\theta] \qquad (B.6)$$

Using worst-case values of $\theta = 40°$, $\alpha = 6.89$ rad/s^2 (derived

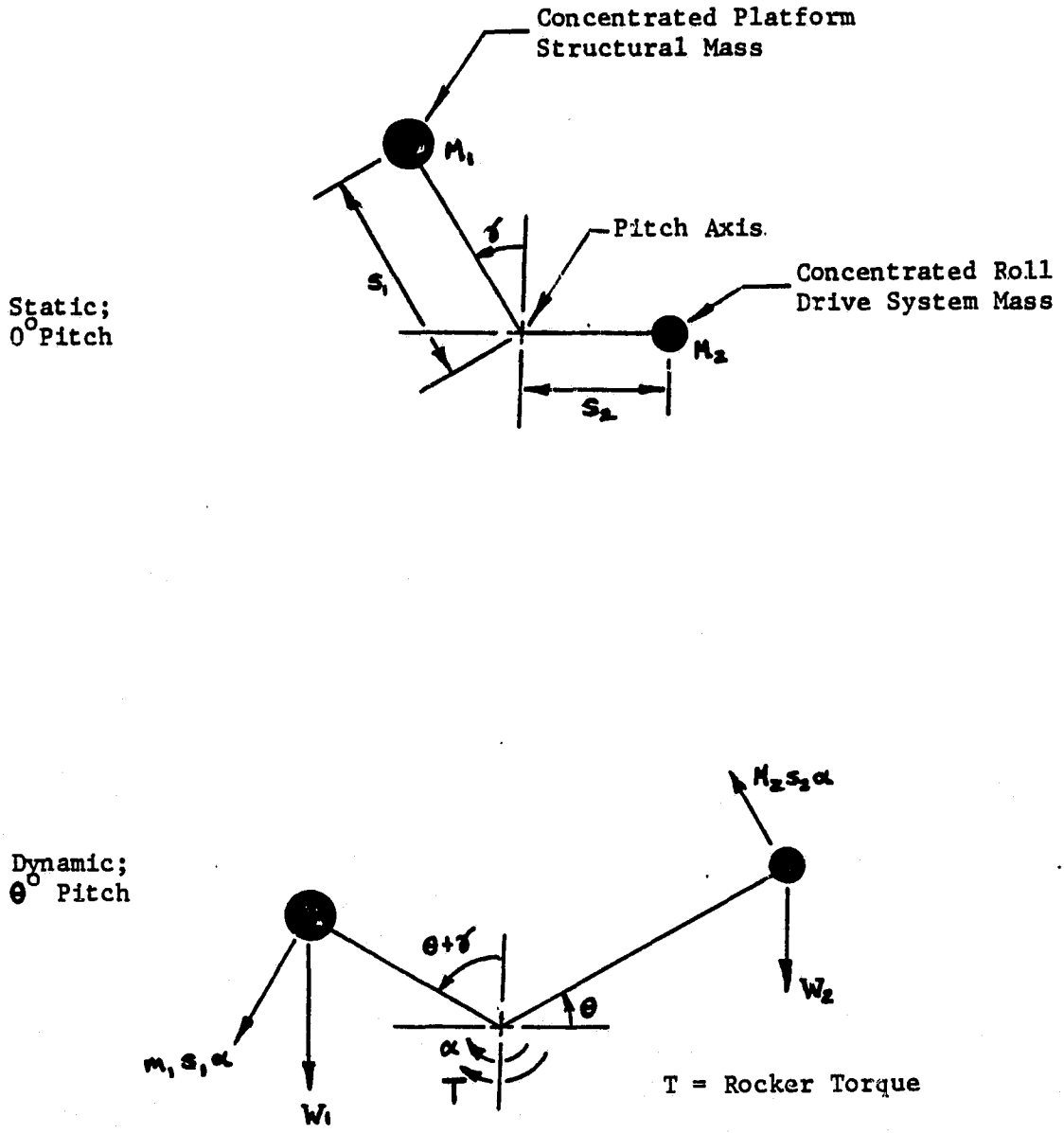

Fig. B.2

Platform Torque Model - Pitch

in Eqns. B.2 - B.5) and estimating the other parameters as

$$W_1 = 50 \text{ lb}$$

$$W_2 = 25 \text{ lb}$$

$$s_1 = 30"$$

$$s_2 = 20"$$

$$\gamma = 30°$$

then Eqn. B.6 gives $T = 2000$ in-lb.

In Eqn. B.6, the second term,

$$W_2 s_2 (a_2 \frac{\alpha}{g} - \cos\theta)$$

represents the contribution of the roll drive system mass to the total required rocker torque. Since this contains a positive and a nagative term, there is a value of the independent variable s_2 which minimizes T for a given pair of values α and θ. To minimize this torque and find the appropriate value of s_2, let

$$\frac{d}{ds_2}(s_2 \frac{2\alpha}{g} - s_2 \cos\theta) = 0$$

which yields

$$s_2 = \frac{g\cos\theta}{2\alpha} \qquad (B.7)$$

This value of s_2, the position of the roll drive system masses, gives the lowest pitch rocker torque. At $\theta = 40°$ and $\alpha = 6.89$ rad/s, this value is $s_2 = 21.5"$, which is the basis for the position in the actual design, approximately 20". Table B.2 lists values of s_2 corresponding to the angular accelerations of Table B.1.

output amplitude (deg.)	crank speed			
	3 rpm	10 rpm	20 rpm	30 rpm
5	22,380	2,011	503	223
10	11,232	994	249	110
15	7,233	650	163	72.2
20	5,600	474	119	52.7
25	4,063	366	91.5	40.7
30	3,236	291	72.8	32.4
35	2,625	236	59	26.2
40	2,148	193	48.3	21.5

Table B.2

Position of roll drive system major masses to minimize pitch torque, in inches behind pitch axis

B.3 Crank Torques

With known values of rocker torque, it is necessary to find the corresponding torques at the crank link. This is done by using the method of instantaneous centers of rotation, which was discussed in Part 3.3.

When the torque figures for both rocker and crank links are plotted against crank angle, the result is a torque profile. The profile for pitch oscillation at 40° and 0.5 cps frequency is shown in Fig. B.3, roll in Fig. B.4.

A horsepower scale is added to the plot by noting that power is the product of torque and speed, specifically

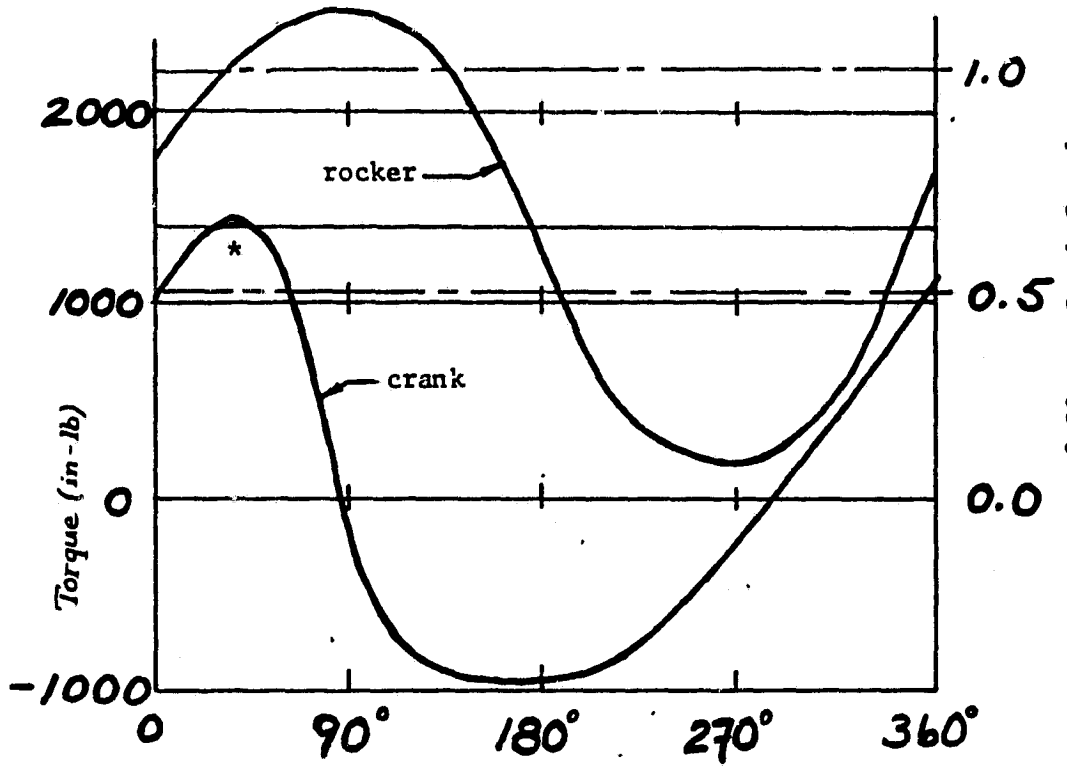

Fig. B.3
Torque & HP Profile -
Pitch: 40° @ 0.5 cps

*Refer to Section B.5 and Fig. B.5

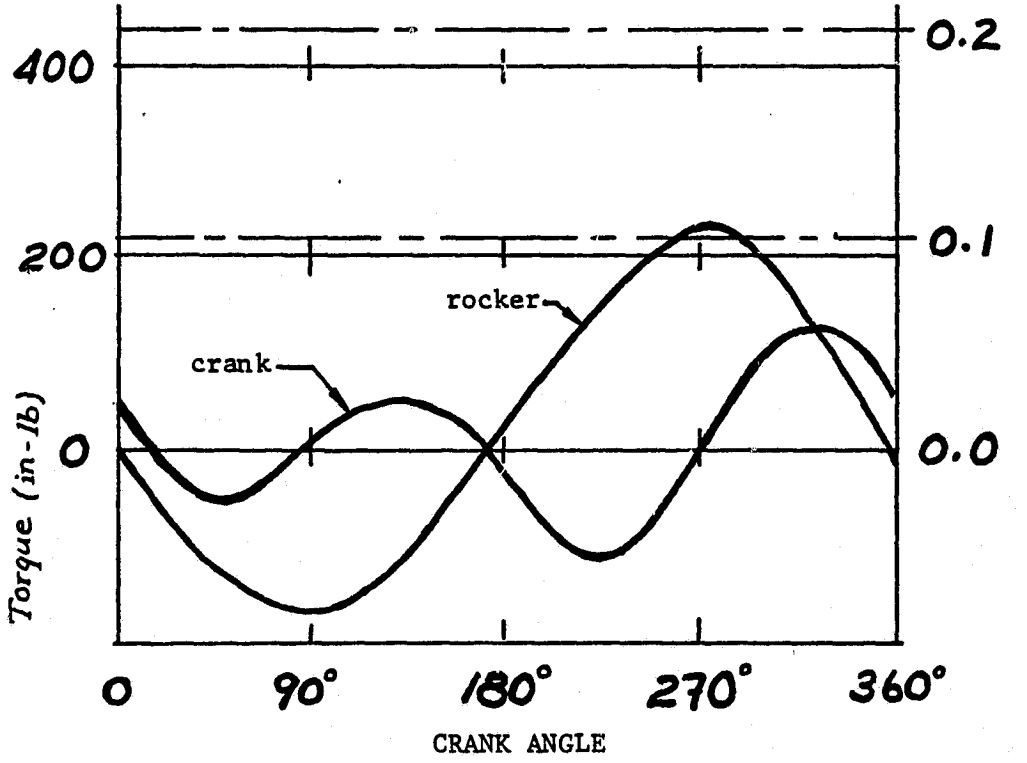

Fig. B.4
Torque & HP Profile -
Roll: 40° @ 0.5 cps

$$hp = \frac{Tn}{63,000}$$

with crank torque, T, in in-lb, and crank speed, n, in rpm. This form of the data simplified motor selection.

B.4 Coupler Forces

Referring again to Fig. B.1, it is safe to consider the forces in the coupler link to be given by

$$F = T/b$$

where T is rocker torque and b is rocker length.

Maximum peak torque in pitch is taken as 2000 in-lb, and 250 in-lb in roll. The corresponding coupler forces are

	T	b	f
pitch	2000 in-lb	6"	333 lb
roll	250 in-lb	4"	63 lb

To design against buckling, Euler buckling criteria are applied, where in the critical load is given by

$$F_c = \frac{\pi^2 EA}{L^2/k^2}$$

where: E = Young's modulus (3×10^7 psi for steel)

A = cross-sectional area in in^2

L = length of link in inches

k = radius of gyration = $(I/A)^{1/2} = [\frac{D_o^2+D_i^2}{16}]^{1/2}$ for cylinder

The data on the two couplers used is tabulated as follows:

	D_o	D_i	L	F_c	F_c/F
pitch	5/8"	7/8"	36"	4860 lb	14.6
roll	1/2"	11/16"	25"	3740 lb	59.4

Obviously the safety margin is very large. In roll the maximum applied load is only 1.7% of the Euler-derived critical load. In fact, the coupler links were sized for convenience in accommodating rod end bearings rather than loading conditions. The radial load limit on the Fafnir sperical rod end bearings used is approximately 2750 lb in pitch and 1900 lb in roll.

B.5 Flywheels

Figure B.3, the pitch torque/power profile, shows the demands on the pitch motor. The characteristic form of the profile is one of extremes, with nearly 100% torque reversals occurring each cycle. This type of load variation might well be controlled by flywheel energy storage.

Referring to Fig. B.3, if a 1/2-hp motor were employed, the motor has more power than required for any instant when the crank curve falls below the 0.5-hp line. During these portions of the cycle energy may be stored in a flywheel, to be used when the curve rises above the 0.5-hp line. The area under the curve and above the line would represent the minimum energy storage required. An appropriate flywheel size is estimated below.

Figure B.5 represents a portion of Fig. B.3, where the crank horsepower curve rises above the 0.5-hp line. If, for ease of integration it is assumed that the portion of the curve in question approxi-

Approximating a sine curve:

let $\phi^* = \pi/2$

$\phi_2 - \phi_1 = 1.22$

then $\phi_1 = 0.96$

$\phi_2 = 2.18$

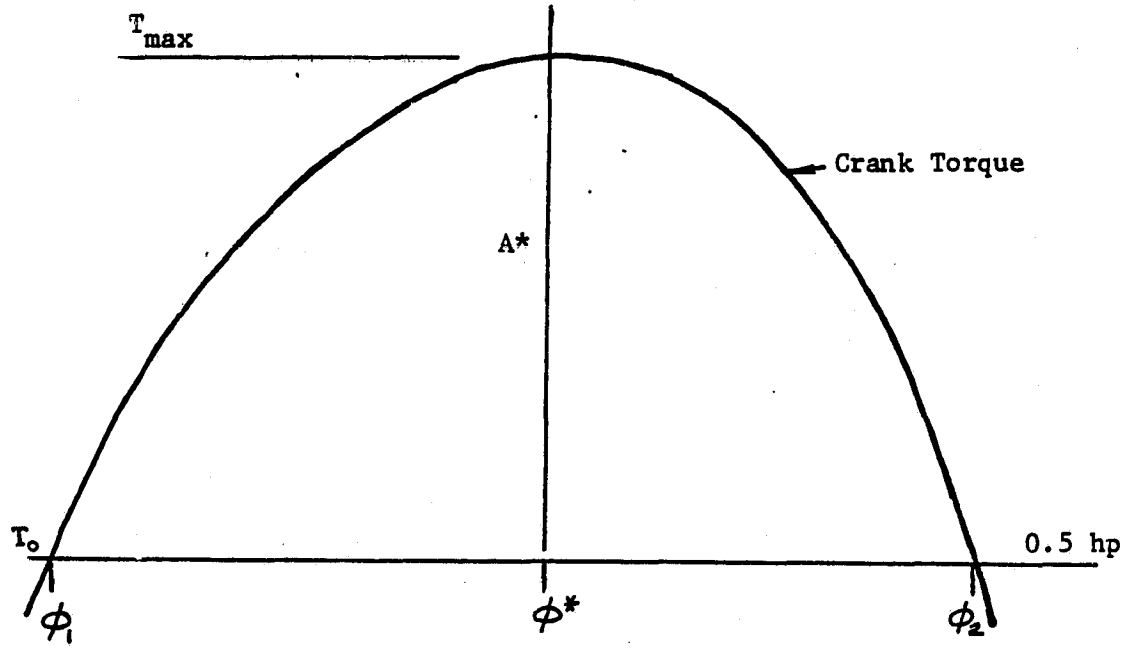

Fig. B.5

Excess Crank Torque

Flywheel Enregy Requirement

mates a sine wave, then the enclosed area is

$$A^* = \int_{\phi_1}^{\phi_2} (T_{max} - T_o) \sin\phi \, d\phi$$

since T_{max} = 2000 in-lb and T_o (1/2-hp @ 1800 rpm) is 1050 in-lb,

$$A^* = -950\cos\phi \Big|_{0.96}^{2.18} = 1090 \text{ in-lb}$$

Flywheel size is characterized by its moment of inertia. Using the value of A* found above, the required moment of inertia is

$$I = A^*/(c\omega_{av}^2)$$

where $c = \frac{\omega_{hi} - \omega_{lo}}{\omega_{av}}$, the coefficient of fluctuation, specifies the amount of allowable speed variation. In the case shown here, if c = 5% and ω_{av} = 1800 rpm = 60 rad/s, then

$$I = 0.6136 \text{ in-lb-s}^2$$

For a disk-type flywheel,

$$I = \frac{Wd^2}{8g} = \frac{\rho\pi d^4 t}{32g}$$

Let $\rho = 0.284$ lb/in^3 be the density of the flywheel (steel), and t = 1.0" be the thickness of the disk. The diameter and weight of the flywheel would be

$$d = 9.6" \qquad W = 20.57 \text{ lb}$$

APPENDIX C

MOTORS AND TRANSMISSIONS

This appendix gives the specifications of the drive system components. Motor characteristics are outlined in Part 3.4 of the text. Gear ratios were chosen on the basis of considerations in Part 3.4 as well. Gear specifications given here which were used in selection deal with dimensions and load ratings of the gears.

C.1 Worm Reduction

Final reduction in both pitch and roll is by high-ratio worm sets. Specifications are listed below.

	Pitch		Roll	
	worm	worm gear	worm	worm gear
ratio	40:1		30:1	
pitch	12		10	
pressure angle	14.5°		14.5°	
center distance	3.833"		3.625"	
input hp	0.17 @ 111 rpm 1.18 @ 1200 rpm		0.19 @ 83 rpm 1.28 @ 900 rpm	
output torque (in-lb)	2771 @ 111 rpm 2037 @ 1200 rpm		2935 @ 83 rpm 2172 @ 900 rpm	
gear	Browning W12-2G	Browning BWG1280-2	Browning WF10A-2G	Browning BWG1060-2
material	hardened and ground steel	bronze	hardened and ground steel	bronze
pitch dia.	1.000"	6.667"	1.250"	6.000"
bore	0.5"	0.75"	0.75"	0.875"
weight	0.2 lb	3.9 lb	0.5 lb	4.0 lb

C.2 Spur Gearing

Primary ratio gearing in the pitch transmission is by spur gears. The specifications:

	Low Range		High Range	
	Driving	Driven	Driving	Driven
ratio	6:1		2:1	
pitch	12		12	
press. angle	20°		14.5°	
gear	Browning YSS1212	Browning YCS12H72	Browning NSS1228	Browning NSS1256
no. teeth	12	72	28	56
pitch diameter	1.0"	6.0"	2.33"	4.667"
outside diameter	1.16"	6.16"	2.50"	4.83"
bore	0.5"	*	0.625"	**
weight	0.2 lb	3.4 lb	1.4 lb	4.4 lb
hp @ rpm	1.31 @ 500	1.45 @ 83	2.35 @ 500	2.71 @ 250

*72 tooth gear uses patented split taper bushing of 1.375" bore
**56 tooth gear is minimum bore hub style, modified to 1.375"

C.3 Gearbelt Drive

Primary ratio gearing in roll is via gearbelts as specified:

	Low Range		High Range	
	Driving	Driven	Driving	Driven
ratio	4.5:1		1.5:1	
pitch	3/8"		3/8"	
center distance	5.7"		5.6"	
belt	Browning 300L		Browning 187L	
width	1"		1"	
pulleys	Browning 16LF100	Browning 72LP100	Browning 16LF100	Browning 24LB100
no. grooves	16	72	16	24
pitch dia.	1.91"	8.594"	1.91"	2.865"
outside dia.	1.88"	8.568"	1.88"	2.835"
bore	0.625"	*	0.625"	**
weight	1.0 lb	2.5 lb	1.0 lb	7.6 lb

*split taper bushing, 1.375" bore
**minimum bore hub, bored to 1.375"

APPENDIX D

SUMMARY OF COST

This appendix summarizes the expenses incurred in the platform program.

D.1 Hardware

Motors	$ 280	
Gearing components	200	
Bearings, pillow blocks, rod ends	450	
Fasteners	200	
Hardware Total		$1,130

D.2 Materials

Approximate total for various quantities of aluminum, mild steel and stainless steel	$ 500

D.3 Labor

Machine shop: one full-time machinist for approximately 20 weeks at	800 hours
Graduate research: 20 hrs/wk for approximately 36 weeks	720
10 hrs/wk for approximately 30 weeks	300
Graduate Total	1,020 hours